

UNCLASSIFIED

AD 414567

DEFENSE DOCUMENTATION CENTER

FOR

SCIENTIFIC AND TECHNICAL INFORMATION

CAMERON STATION, ALEXANDRIA, VIRGINIA

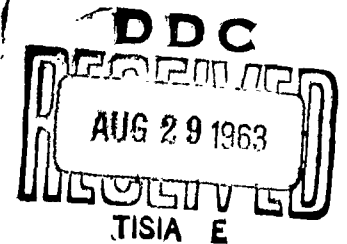


UNCLASSIFIED

NOTICE: When government or other drawings, specifications or other data are used for any purpose other than in connection with a definitely related government procurement operation, the U. S. Government thereby incurs no responsibility, nor any obligation whatsoever; and the fact that the Government may have formulated, furnished, or in any way supplied the said drawings, specifications, or other data is not to be regarded by implication or otherwise as in any manner licensing the holder or any other person or corporation, or conveying any rights or permission to manufacture, use or sell any patented invention that may in any way be related thereto.

AEDC-TDR-63-163

**PRESSURE DISTRIBUTION AND FLOW
VISUALIZATION TESTS OF A 1.5 ELLIPTIC CONE
AT MACH 10**



By

R. L. Palko and A. D. Ray
von Kármán Gas Dynamics Facility
ARO, Inc.

TECHNICAL DOCUMENTARY REPORT NO. AEDC-TDR-63-163

August 1963

Program Element 62405334/1366, Task 136607

(Prepared under Contract No. AF 40(600)-1000 by ARO, Inc.,
contract operator of AEDC, Arnold Air Force Station, Tenn.)

**ARNOLD ENGINEERING DEVELOPMENT CENTER
AIR FORCE SYSTEMS COMMAND
UNITED STATES AIR FORCE**

CATALOGED BY DDC
AS AD 14567
414567
ARNOLD ENGINEERING DEVELOPMENT CENTER

NOTICES

Qualified requesters may obtain copies of this report from DDC, Cameron Station, Alexandria, Va. Orders will be expedited if placed through the librarian or other staff member designated to request and receive documents from DDC.

When Government drawings, specifications or other data are used for any purpose other than in connection with a definitely related Government procurement operation, the United States Government thereby incurs no responsibility nor any obligation whatsoever; and the fact that the Government may have formulated, furnished, or in any way supplied the said drawings, specifications, or other data, is not to be regarded by implication or otherwise as in any manner licensing the holder or any other person or corporation, or conveying any rights or permission to manufacture, use, or sell any patented invention that may in any way be related thereto.

PRESSURE DISTRIBUTION AND FLOW
VISUALIZATION TESTS OF A 1.5 ELLIPTIC CONE
AT MACH 10

By
R. L. Palko and A. D. Ray
von Kármán Gas Dynamics Facility
ARO, Inc.
a subsidiary of Sverdrup and Parcel, Inc.

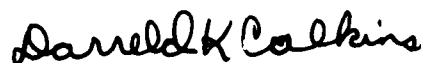
August 1963
ARO Project No. VC0330

ABSTRACT

Results are presented for tests conducted on a 1.5 elliptic cone to determine the pressure distribution, flow streamlines, and shock wave shape at high angles of attack. The tests were performed at a Mach number of 10 and a free-stream unit Reynolds number of 1.6×10^6 per foot. The angle-of-attack range was from 0 to 60 deg. The model was oriented both with the major and with the minor axis of the ellipse located in the pitch plane.

PUBLICATION REVIEW

This report has been reviewed and publication is approved.



Darreld K. Calkins
Major, USAF
AF Representative, VKF
DCS/Test



Jean A. Jack
Colonel, USAF
DCS/Test

CONTENTS

	<u>Page</u>
ABSTRACT.	iii
NOMENCLATURE.	viii
1.0 INTRODUCTION	1
2.0 APPARATUS	
2.1 Wind Tunnel	1
2.2 Model and Support	2
2.3 Instrumentation.	2
3.0 PROCEDURE	
3.1 Test Conditions.	3
3.2 Test Procedure.	4
3.3 Data Reduction	4
4.0 RESULTS AND DISCUSSION	5
REFERENCES	6

ILLUSTRATIONS

Figure

1.	Details of the 50-Inch Mach 10 Tunnel (C)	
	a. Tunnel Assembly	9
	b. Tunnel Test Section	9
2.	Model Detail	10
3.	Model Instrumentation	
	a. Pressure Tap Location.	11
	b. Nondimensional Point Coordinates of Pressure Taps	12
4.	Model Installation Viewed from Top of Tunnel	13
5.	Comparison between Measured Data and Newtonian Theory for the 0-deg Ray of Configuration 1	14
6.	Pressure Distribution along 0-deg Ray of Configuration 1	15
7.	Pressure Distribution along 180-deg Ray of Configuration 1	16
8.	Pressure Distribution along 100-deg Ray of Configuration 2	17

<u>Figure</u>		<u>Page</u>
9.	Comparison between Measured Data and Newtonian Theory for Cross Sections 3.0, 6.5, and 11.5 of Configuration 1.	18
10.	Comparison between Measured Data and Newtonian Theory for Cross Sections 3.0, 6.5, and 11.5 of Configuration 2.	19
11.	Pressure Distribution for Cross Section 3.0 of Configuration 1.	20
12.	Pressure Distribution for Cross Section 6.5 of Configuration 1	
	a. S of 0 to 0.5	21
	b. S of 0.25 to 0.5.	22
13.	Pressure Distribution for Cross Section 11.5 of Configuration 1.	23
14.	Pressure Distribution for Cross Section 3.0 of Configuration 2.	24
15.	Pressure Distribution for Cross Section 6.5 of Configuration 2.	25
16.	Pressure Distribution for Cross Section 11.5 of Configuration 2.	26
17.	Effect of Angle of Attack on Point of Flow Separation.	27
18.	Oil Flow Photographs of Configuration 1 .	
	a. $\alpha = 0$ deg	28
	b. $\alpha = 10$ deg	29
	c. $\alpha = 20$ deg	30
	d. $\alpha = 30$ deg	31
	e. $\alpha = 40$ deg	32
	f. $\alpha = 50$ deg	33
	g. $\alpha = 60$ deg	34
19.	Oil Flow Photographs of Configuration 2	
	a. $\alpha = 0$ deg	35
	b. $\alpha = 10$ deg	36
	c. $\alpha = 20$ deg	37
	d. $\alpha = 30$ deg	38
	e. $\alpha = 40$ deg	39
	f. $\alpha = 50$ deg	40
	g. $\alpha = 60$ deg	41

<u>Figure</u>		<u>Page</u>
20.	Shadowgraphs of Configuration 1	
	a. $\alpha = 0$ deg	42
	b. $\alpha = 10$ deg	43
	c. $\alpha = 20$ deg	44
	d. $\alpha = 30$ deg	45
	e. $\alpha = 40$ deg	46
	f. $\alpha = 50$ deg	47
	g. $\alpha = 60$ deg	48
21.	Shadowgraphs of Configuration 2	
	a. $\alpha = 0$ deg	49
	b. $\alpha = 10$ deg	50
	c. $\alpha = 20$ deg	51
	d. $\alpha = 30$ deg	52
	e. $\alpha = 40$ deg	53
	f. $\alpha = 50$ deg	54
	g. $\alpha = 60$ deg	55

NOMENCLATURE

C_p	Pressure coefficient, $(p - p_\infty)/q_\infty$
c	Semimajor axis of elliptic cone, Configuration 1 (7.768 in.) Semiminor axis of elliptic cone, Configuration 2 (5.178 in.)
L	Model length, 14.303 in.
p	Local static pressure, psia
p_o	Stagnation pressure, psia
p_∞	Free-stream static pressure, psia
q_∞	Free-stream dynamic pressure, psia
S	$\phi / 360$ deg
\bar{S}	x/L
T_o	Stagnation temperature, °R
x	Distance from nose to pressure tap, measured along centerline of model, in.
y_s	Half the distance between flow separation lines on the ellipse at the base
α	Angle of attack, deg
θ_s	Angle measured around base ellipse from horizontal base axis to flow separation line on cone
ϕ	Angle to pressure taps around model, measured clockwise looking upstream with $\phi = 0$ at bottom of Configuration 1

1.0 INTRODUCTION

Tests were conducted on a 1.5 elliptic cone in cooperation with the Aeronautical Systems Division (ASD), Air Force Systems Command (AFSC), to determine the pressure distribution, flow streamlines, and shock wave shape at high angles of attack. The tests were performed in the 50-Inch Mach 10 Tunnel (C) of the von Kármán Gas Dynamics Facility (VKF), Arnold Engineering Development Center (AEDC), AFSC, during the period from April 11 to 17, 1963.

Pressure data, oil flow photographs, and shadowgraphs were obtained at a free-stream unit Reynolds number of 1.6×10^6 per foot with the model oriented both with the major and with the minor axis of ellipse located in the pitch plane. The angle-of-attack range investigated was from 0 to 60 deg in 10-deg increments.

The results of these tests are presented.

2.0 APPARATUS

2.1 WIND TUNNEL

The 50-Inch Mach 10 Tunnel (C) is an axisymmetric, continuous flow, variable-density, hypersonic wind tunnel. Because of changes in the boundary-layer thickness caused by changing pressure levels, the contoured nozzle produces an average test section Mach number which varies from 10.0 at a stagnation pressure of 200 psia to 10.2 at 2000 psia. Details of the tunnel are shown in Fig. 1.

Stagnation pressures up to approximately 2000 psia are supplied to the tunnel by the VKF 92,500-hp compressor system. The air is selectively valved through the compressor system, high pressure driers, propane-fired heater, and the 12,000-kw electric heater. The propane-fired heater preheats the air to 700°F for the 50-Inch Mach 10 Tunnel (C). The 12,000-kw electric heater is required to increase the air temperature to a maximum of 1450°F to prevent liquefaction in the test section. After heating, the air flows through the nozzle, test section, diffuser, cooler, and back into the compressor system.

A unique feature of the tunnel is the model installation chamber below the test section which allows the entire pitch mechanism, sting,

Manuscript received July 1963.

and model to be lowered out of the tunnel. When the model is in the retracted position, the fairing doors and the safety doors can be closed (Fig. 1), and the tank can be entered for model changes while the tunnel is running. When the model is in the test section, only the fairing doors are closed, and the tank remains at tunnel static pressure.

A complete description of the tunnel is given in Ref. 1.

2.2 MODEL AND SUPPORT

The model was a 1.5 elliptic cone with a major base axis of 7.768 in., minor base axis of 5.178 in., and a length of 14.303 in. (Fig. 2). The model was fabricated of stainless steel by Grumman Aircraft Co. for previous testing in the 50-Inch Mach 8 Tunnel (B) (see Ref. 2).

The instrumentation consisted of 53 pressure taps located on the model as shown in Fig. 3.

To test the model through the desired angle-of-attack range from 0 to 60 deg it was necessary to use three different prebent stings. Roll orientation was performed by rolling the model on the sting in front of the sting prebend.

The model was oriented in two positions which were designated Configurations 1 and 2 (Fig. 2). For Configuration 1 the minor axis of the ellipse was oriented in the pitch plane, and for Configuration 2 the major axis was oriented in the pitch plane.

Figure 4 shows Configuration 1 installed in the tunnel as viewed from the top.

2.3 INSTRUMENTATION

2.3.1 Pressure Instrumentation

The pressure data system is a nine-channel unit which uses 12-position Giannini pressure switching valves. The total capability is 99 model measurements with the first position of each pressure switching valve being used for transducer calibration.

Each channel includes two pressure measuring transducers (referenced to hard vacuum). The two measuring transducers, a ± 1 -psid unit

and a 0- to 15-psid unit, are switched in and out of the system automatically to allow measuring to the best available precision. If the sensed pressure level is above 15 psia, the reference side of the 15-psid transducer is vented to atmosphere to extend the measuring range.

The measuring system is of the Wiancko frequency modulation type. Precision frequency modulation oscillators, frequency multipliers, binary counters, and a time base generator operate in conjunction with the transducers to obtain a differential count of 10,000. The resulting resolution is 0.0002 psi for the 1-psi transducer and 0.0015 psi for the 15-psid transducers. The accumulated count is stored in the binary counters, read out serially by the ERA scanner, and punched on paper tape.

2.3.2 Photographic Instrumentation

The oil flow photographic system consisted of two panels on which were mounted banks of ultraviolet fluorescent lamps. These panels were mounted over the windows of the top and operating side of the tunnel test section. The 35-mm sequence cameras were mounted on the panels and used to record the flow patterns on the model.

A conventional, short range, divergent ray, spark shadowgraph system was used to obtain the shadowgraph pictures. The film pack was mounted directly against the window frame, and the film was automatically advanced with the recording of each photograph.

2.3.3 General

The tunnel stagnation pressures and temperatures were measured in the stilling chamber. A 2500-psid transducer, referenced to vacuum, was used to measure the stagnation pressure, and a chromel-alumel thermocouple was used for the stagnation temperature measurement.

3.0 PROCEDURE

3.1 TEST CONDITIONS

The tests were conducted at a nominal Mach number of 10 at a stagnation pressure of 1285 psia, which corresponds to a free-stream unit Reynolds number of 1.6×10^6 per foot. The stagnation temperature was approximately 1870°R which was sufficient to prevent liquefaction of the air in the test section.

3.2 TEST PROCEDURE

3.2.1 Pressure Measurement

At pre-selected angles of attack, pressure distribution data were recorded on punched paper tape for subsequent computer reduction. The angle-of-attack range was from 0 to 60 deg in 10-deg increments for both configurations.

3.2.2 Photographic Procedure

To obtain the oil flow data, Zyglo oil was used. Before each photographic sequence the model was cleaned and sprayed with the fluorescent oil. At a pre-set angle of attack the model was injected into the tunnel and the cameras started. The model was allowed to remain in the tunnel until the flow pattern of the oil was completely established. When the model was removed from the tunnel, it was cooled with high pressure air and the sequence was repeated.

The shadowgraph pictures were obtained by injecting the model into the tunnel at a pre-set angle of attack and the photographs taken when the model reached tunnel centerline. In order not to expose the film from the model glow when it became hot, it was necessary to return the model to the tank after each photograph for cooling.

The angle-of-attack range during the oil flow and shadowgraph phases was the same as for the pressure phase of the test.

3.3 DATA REDUCTION

The data reduction was performed with the ERA 1102 digital computer. The pressure distribution data were tabulated in the form p/p_∞ and $C_p = (p - p_\infty)/q_\infty$.

The free-stream properties of the airstream were calculated assuming an isentropic expansion process of a Beattie-Bridgeman gas with variable specific heats following the method of Ref. 3. Empirical correction factors of the form

$$\frac{(p_\infty/p_o)_{\text{real}}}{(p_\infty/p_o)_{\text{ideal}}} = f(p_o, T_o)$$

were calculated to facilitate data reduction.

4.0 RESULTS AND DISCUSSION

The purpose of the tests was to determine the pressure distribution, flow streamlines, and shock wave shape on a 1.5 elliptic cone at high angles of attack. To accomplish these objectives pressure data, oil flow photographs, and shadowgraph pictures were obtained.

Figures 5 through 16 present the pressure distributions for Configurations 1 and 2 through the angle-of-attack range. A comparison of the measured data along the bottom row of pressure taps of Configuration 1 (0-deg ray) for the aft three stations, with Newtonian theory is shown in Fig. 5. This comparison shows that the theoretical estimates are in general agreement with the experimental values at these pitch angles.

A presentation of the pressure distributions along this ray is given in Fig. 6. A very peculiar bump becomes evident in the distributions near the nose of the model at an angle of attack of 20 deg and increases with angle of attack. This bump is associated with flow separation which was revealed by oil flow studies which will be covered in later discussion.

Figure 7 presents the pressure distributions for the top row for Configuration 1 (180-deg ray). Here again the data become erratic near the nose at angles of attack above 20 deg. It is also shown that pressures at the aft stations decrease with angle of attack between $\alpha = 0$ and 20 deg and then increase with angle of attack above 20 deg.

Figure 8 shows the results measured along the row nearest the bottom of the model for Configuration 2 (the 100-deg ray which was 10 deg off the bottom centerline for Configuration 2). Here again the bump in the pressure distributions occurs near the nose and becomes evident at an angle of attack of 10 deg.

A comparison of experimental data and Newtonian theory for cross sections $x = 3.0$, 6.5 , and 11.5 in. is shown in Figs. 9 and 10 for Configurations 1 and 2, respectively. Here again the simple theory agrees reasonably well with the experimental results.

Figures 11 through 16 show the pressure distributions for cross sections $x = 3.0$, 6.5 , and 11.5 in. for both Configurations 1 and 2. Figure 12b shows the distributions for the top of Configuration 1 at cross section $x = 6.5$ in. on an expanded scale, and it is noted that the break in the pressure distributions appears near the location where separation occurs, as shown in Fig. 17.

To study the flow streamlines over the model, a complete series of oil flow tests were made and the results of these tests are shown in Figs. 17, 18, and 19.

Jorgensen observed (in Ref. 4) from oil flow and vapor screen studies that a pair of symmetrical vortices start at the nose and trace a linear path to the base at a Mach number of 1.97. These vortices increased in size with travel from the nose to the base. The flow separation lines from which the vortices are fed also trace an essentially linear path along the model surface.

The photographs shown in Figs. 18 and 19 clearly reveal similar lines of flow separation and indicate the presence of similar vortices at Mach 10 (see Fig. 18d). The effect of model angle of attack on the point at which flow separation occurs is shown in Fig. 17.

Further analysis and observations made during the test also reveal the vortex traces. Figure 18 shows that for Configuration 1 the vortex traces extend to the base of the model up to and including an angle of attack of 30 deg. However, at angles of attack above 30 deg the vortices separate from the model before reaching the base. Figures 18e, f, and g show that the vortices separate from the body at approximately $L/2$ for $\alpha = 40$ deg, $L/3$ for $\alpha = 50$ deg, and either do not form or do not attach at $\alpha = 60$ deg.

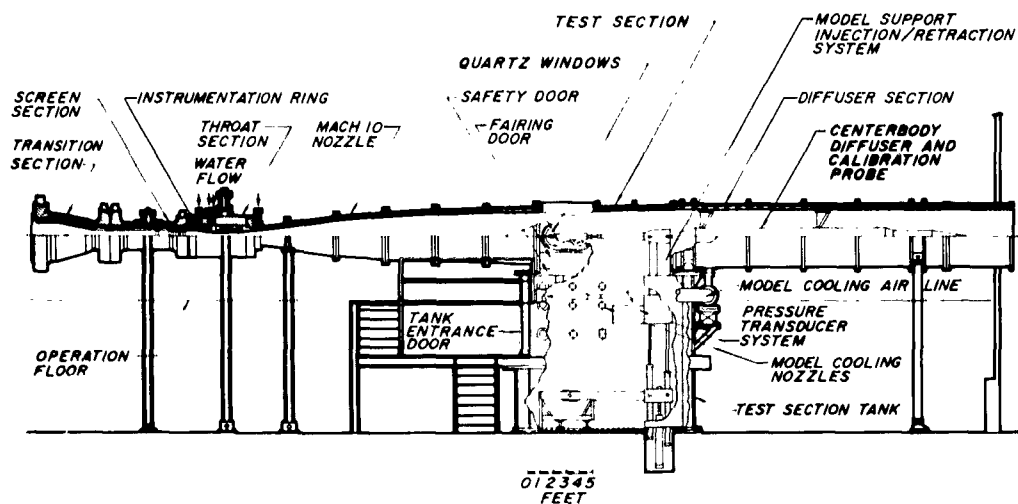
The same observations were made for Configuration 2 (Fig. 19); however, the vortices separation does not occur as quickly. Figures 19e, f, and g reveal that the separation occurs at approximately $3L/4$ for $\alpha = 40$ deg, $L/2$ for $\alpha = 50$ deg, and $L/4$ for $\alpha = 60$ deg.

To determine the shock wave shape, shadowgraph pictures were taken for both configurations through the complete angle-of-attack range. These photographs are presented in Figs. 20 and 21.

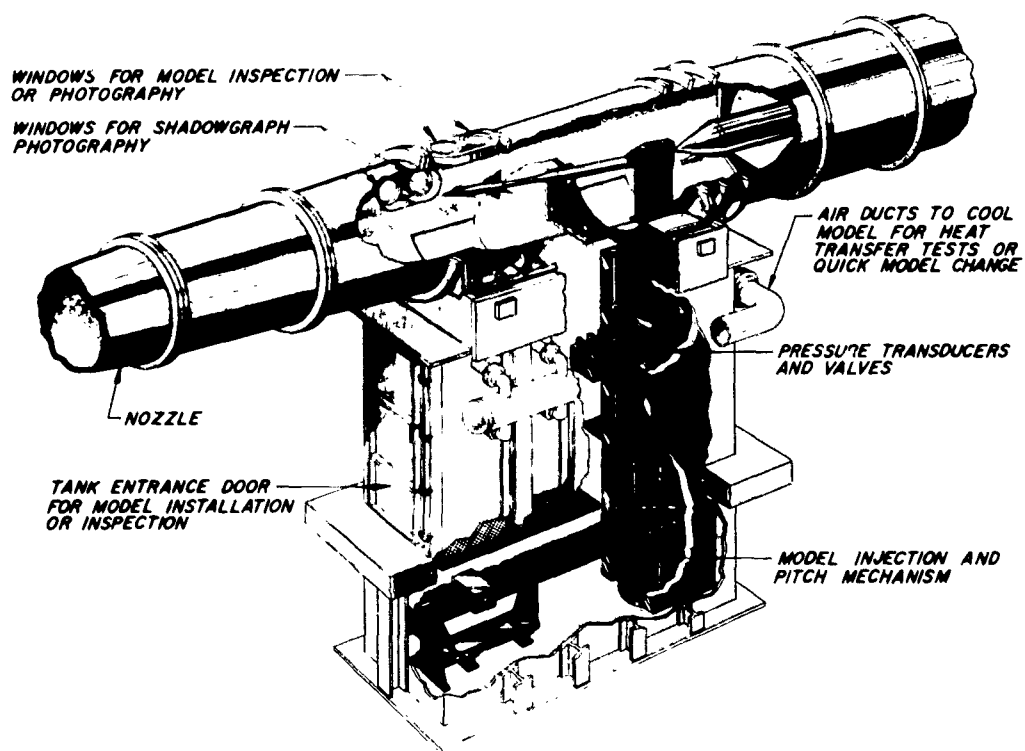
REFERENCES

1. Test Facilities Handbook, (5th Edition). "von Kármán Gas Dynamics Facility, Vol. 4." Arnold Engineering Development Center, July 1963.
2. Randall, R. E., Bell, D. R., and Burk, J. L. "Pressure Distribution Tests of Several Sharp Leading Edge Wings, Bodies, and Body-Wing Combinations at Mach 5 and 8." AEDC-TN-60-173, September 1960

3. Randall, R. E. "Thermodynamic Properties of Air: Tables and Graphs Derived from the Beattie-Bridgeman Equations of State Assuming Variable Specific Heats." AEDC-TR-57-8, August 1957.
4. Jorgensen, Leland H. "Elliptic Cones Alone and with Wings at Supersonic Speeds." NACA-TN-4045, October 1957.



a. Tunnel Assembly



b. Tunnel Test Section

Fig. 1 Details of the 50-Inch Mach 10 Tunnel (C)

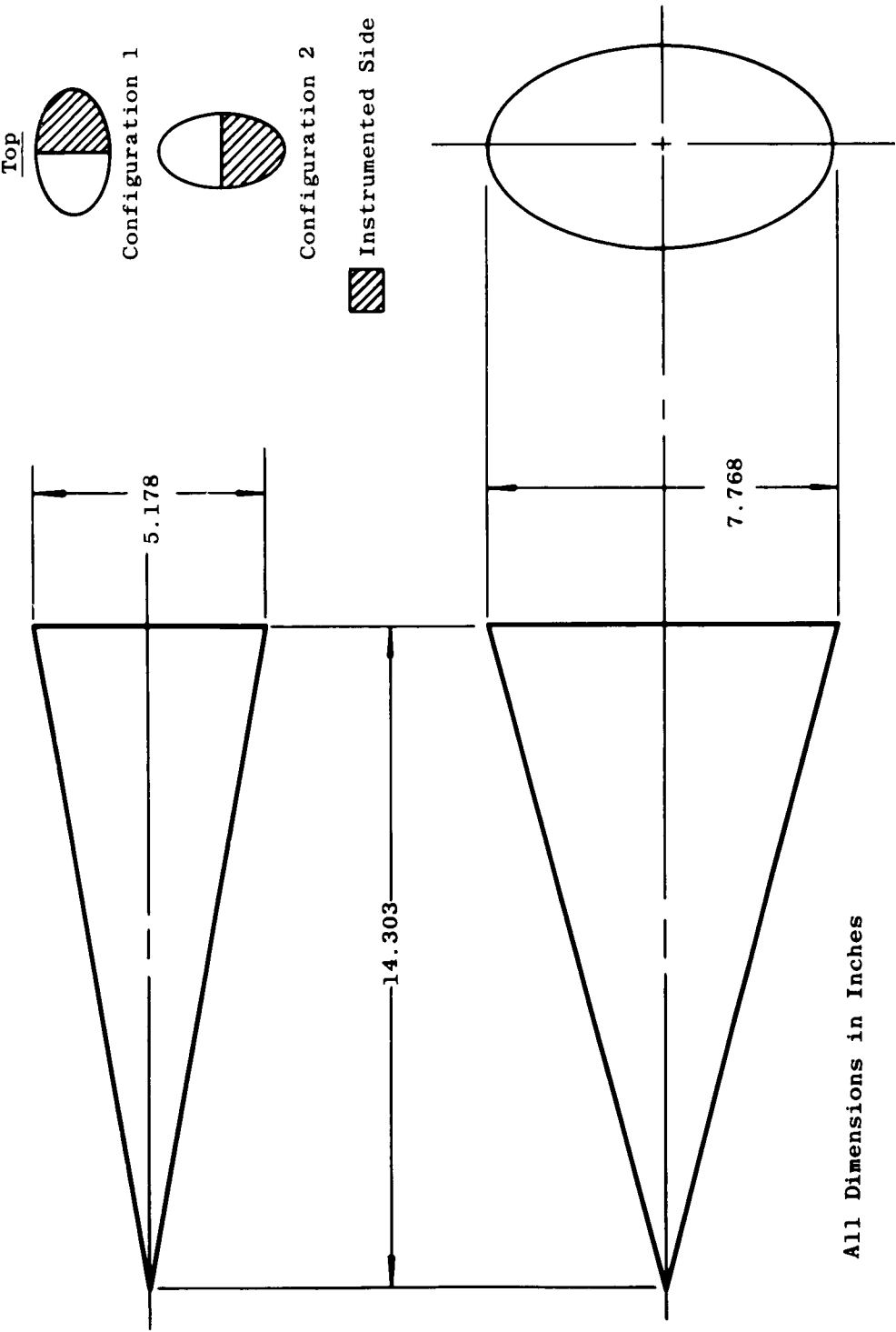
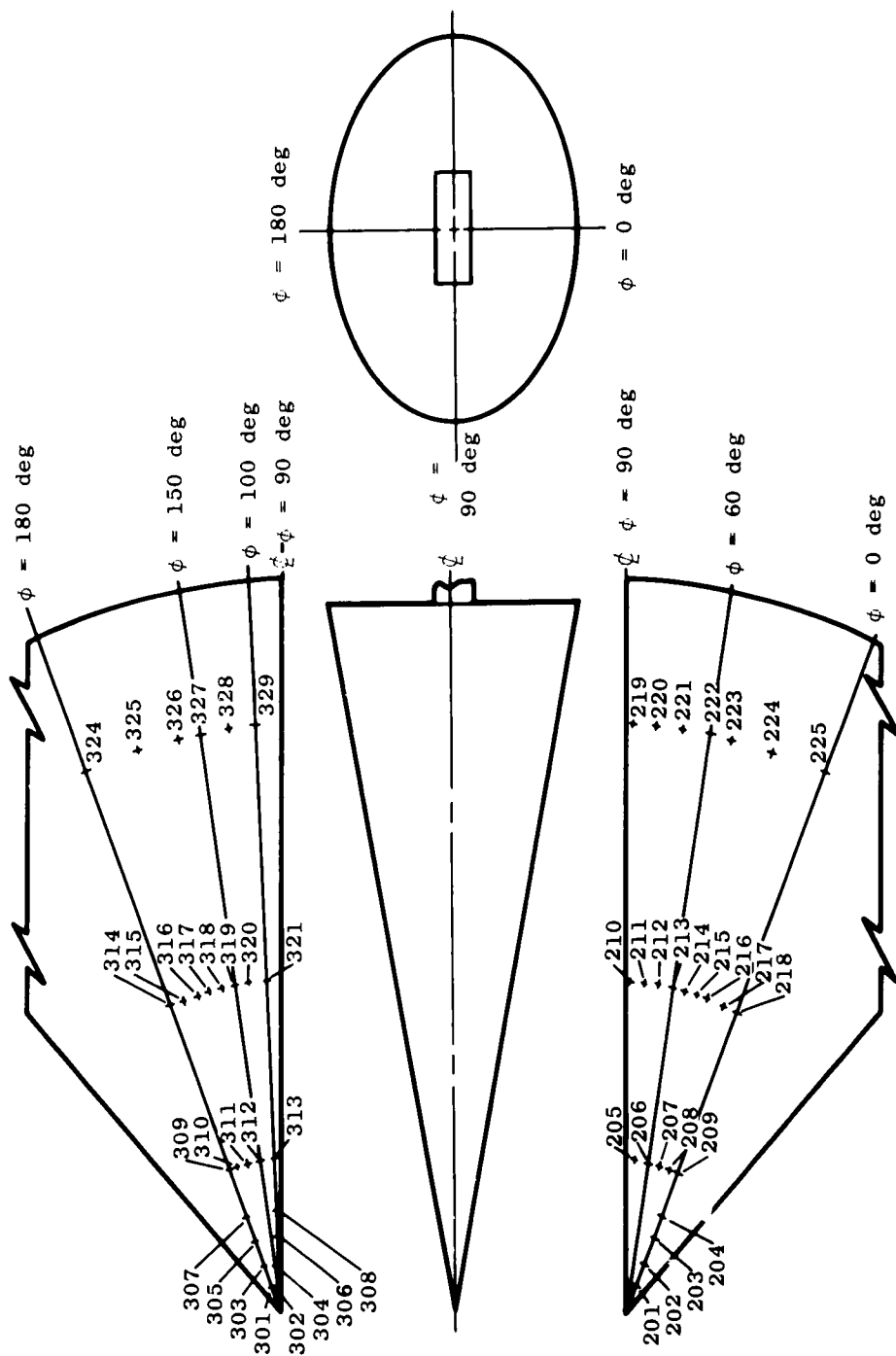


Fig. 2 Model Detail

All Dimensions in Inches



a. Pressure Tap Location

Fig. 3 Model Instrumentation

Cross Section x = 3.0 in.	
Tap No.	S
209	0.0000
208	0.0417
207	0.1111
206	0.1667
205	0.2222
313	0.2778
312	0.3333
311	0.3889
310	0.4583
309	0.5000

$$S = \phi/360 \text{ deg}$$

$$\bar{S} = x/L$$

$$L = 14.303 \text{ in.}$$

Cross Section x = 6.5 in.	
Tap No.	S
218	0.0000
217	0.0417
216	0.0833
215	0.1111
214	0.1389
213	0.1667
212	0.1944
211	0.2222
210	0.2458
322	0.2542
321	0.2778
320	0.3056
319	0.3333
318	0.3611
317	0.3889
316	0.4167
315	0.4583
314	0.5000

Cross Section x = 11.5 in.	
Tap No.	S
225	0.0000
224	0.0833
223	0.1389
222	0.1667
221	0.1944
220	0.2222
219	0.2458
329	0.2778
328	0.3056
327	0.3333
326	0.3611
325	0.4167
324	0.5000

Lower Surface $\phi = 60 \text{ deg}$	
Tap No.	\bar{S}
206	0.2097
213	0.4545
222	0.8040

Upper Surface $\phi = 100 \text{ deg}$	
Tap No.	\bar{S}
302	0.0350
304	0.0699
306	0.1049
308	0.1398
313	0.2097
321	0.4545
329	0.8040

Upper Surface $\phi = 180 \text{ deg}$	
Tap No.	\bar{S}
301	0.0350
303	0.0699
305	0.1049
307	0.1398
309	0.2097
314	0.4545
324	0.8040

Upper Surface $\phi = 150 \text{ deg}$	
Tap No.	\bar{S}
312	0.2097
319	0.4545
327	0.8040

Cross Section - $\phi = 0 \text{ deg}$			
Tap No.	S	Tap No.	S
201	0.0350	209	0.2097
202	0.0699	218	0.4545
203	0.1049	225	0.8040
204	0.1398		

b. Nondimensional Point Coordinates of Pressure Taps

Fig. 3 Concluded

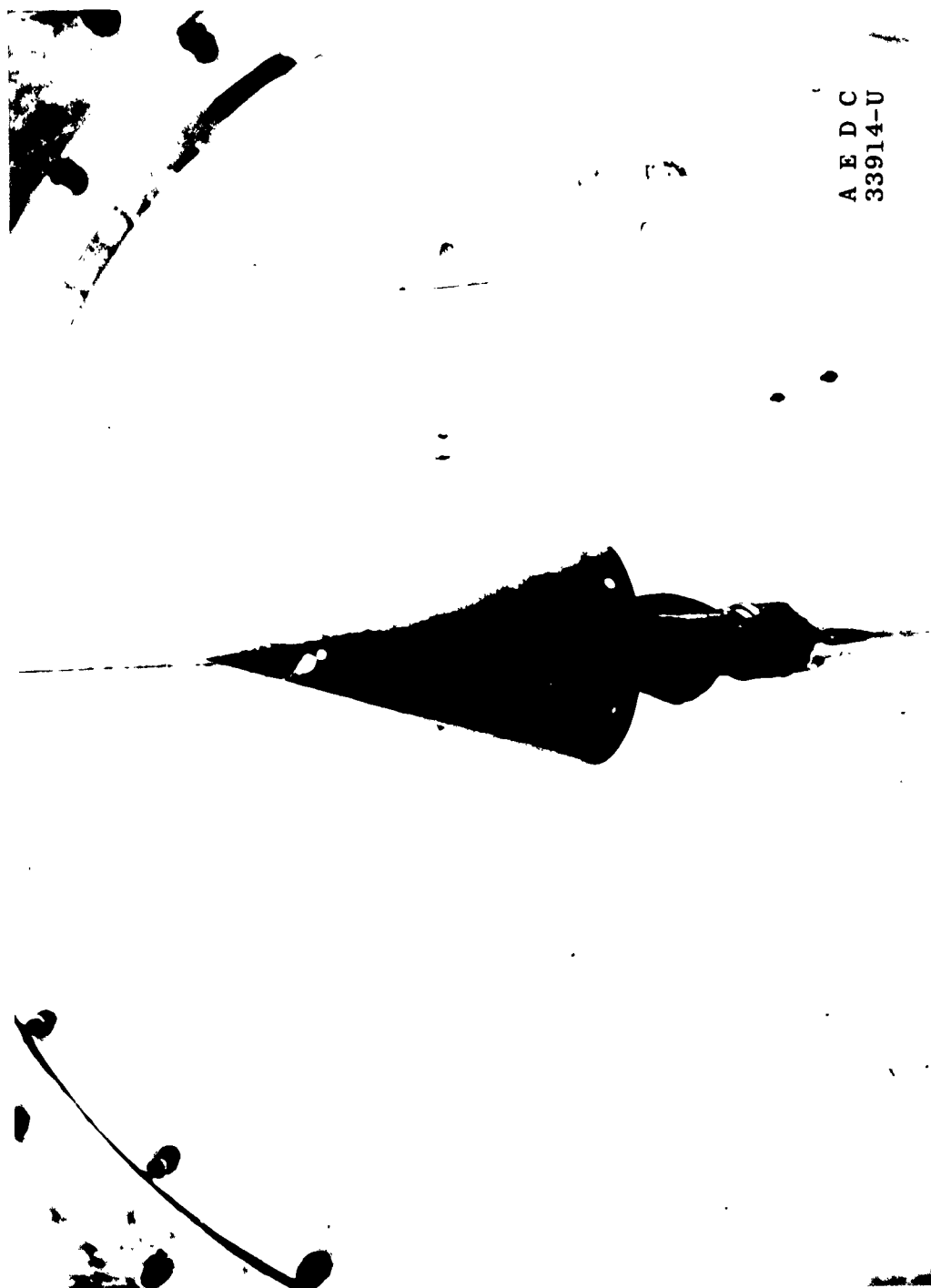


Fig. 4 Model Installation Viewed from Top of Tunnel

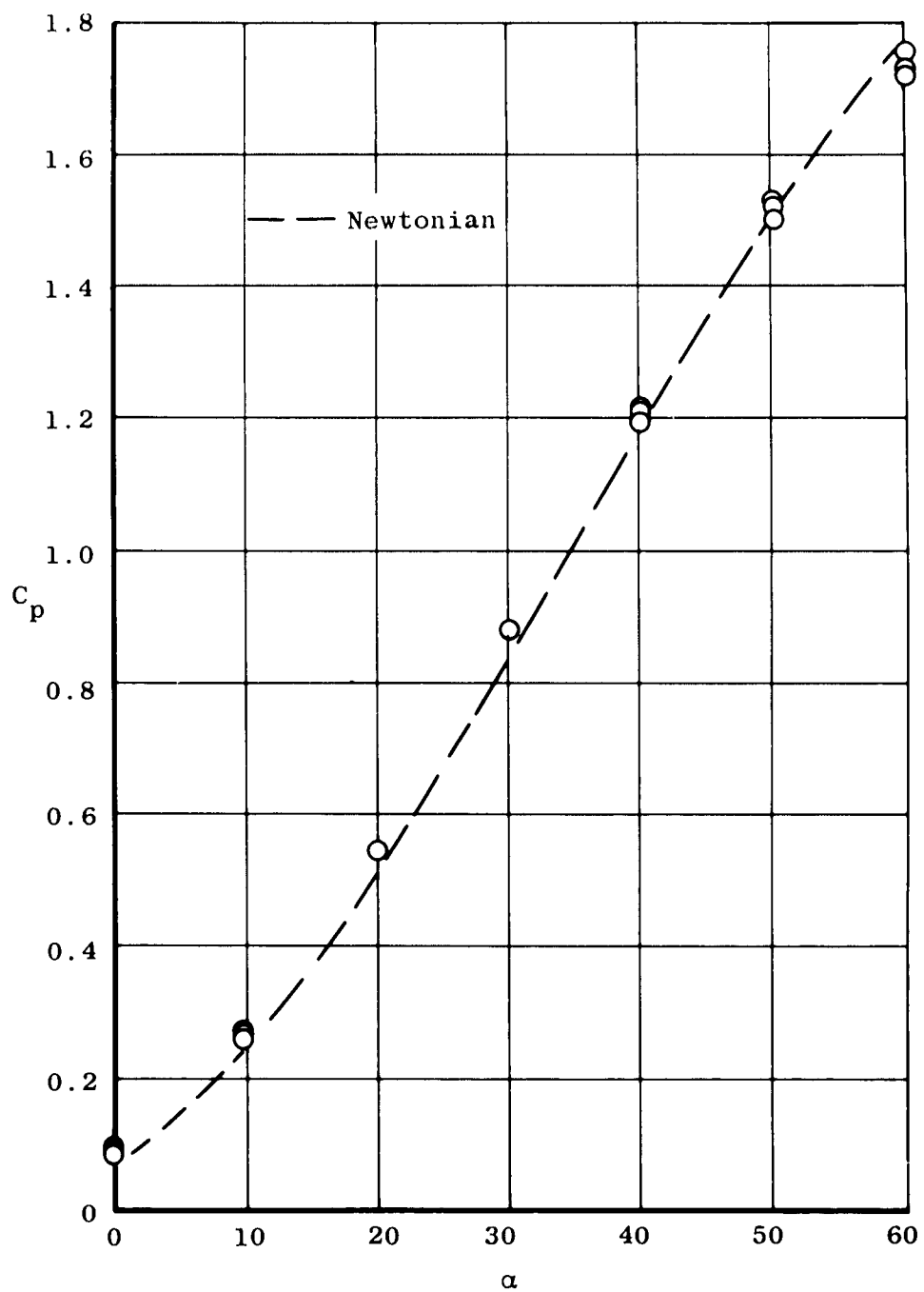


Fig. 5 Comparison between Measured Data and Newtonian Theory for the 0-deg Ray of Configuration 1

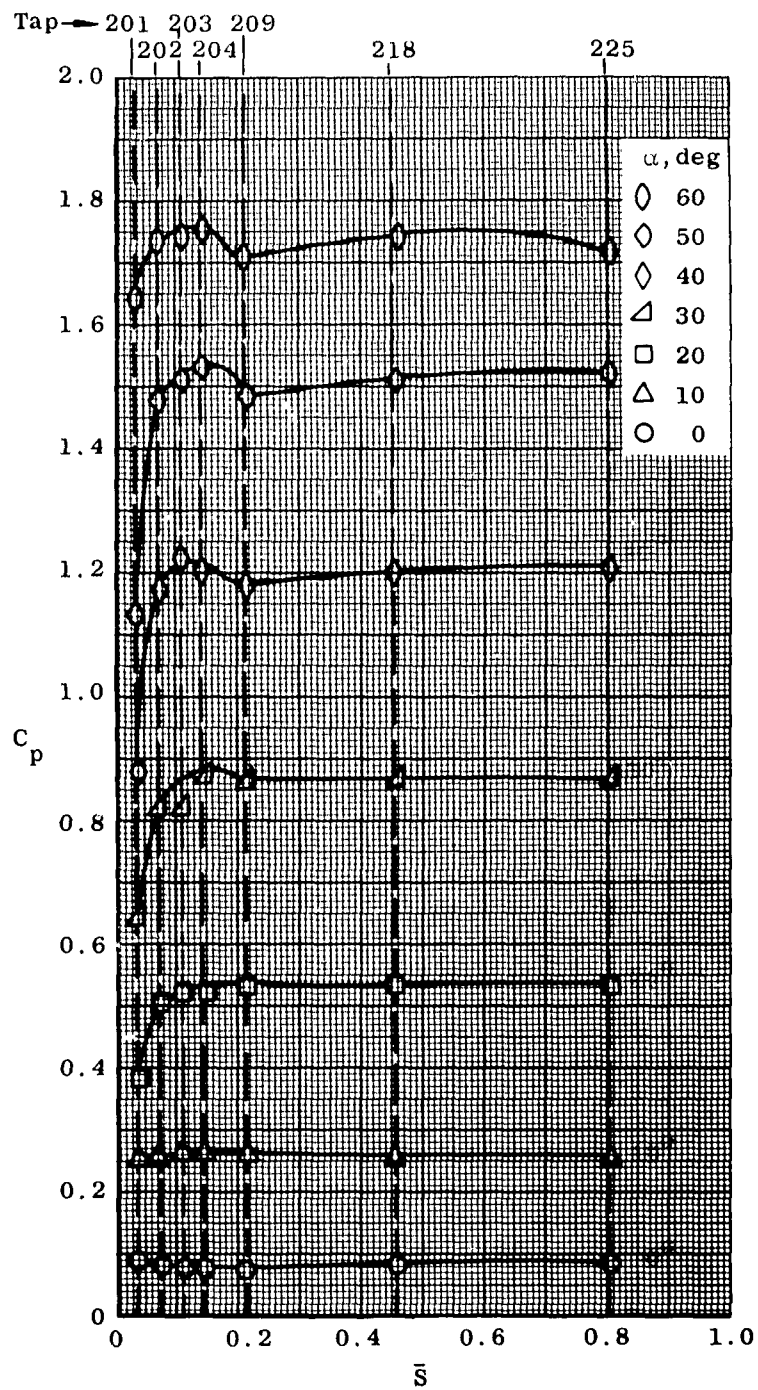


Fig. 6 Pressure Distribution along 0-deg Ray of Configuration 1

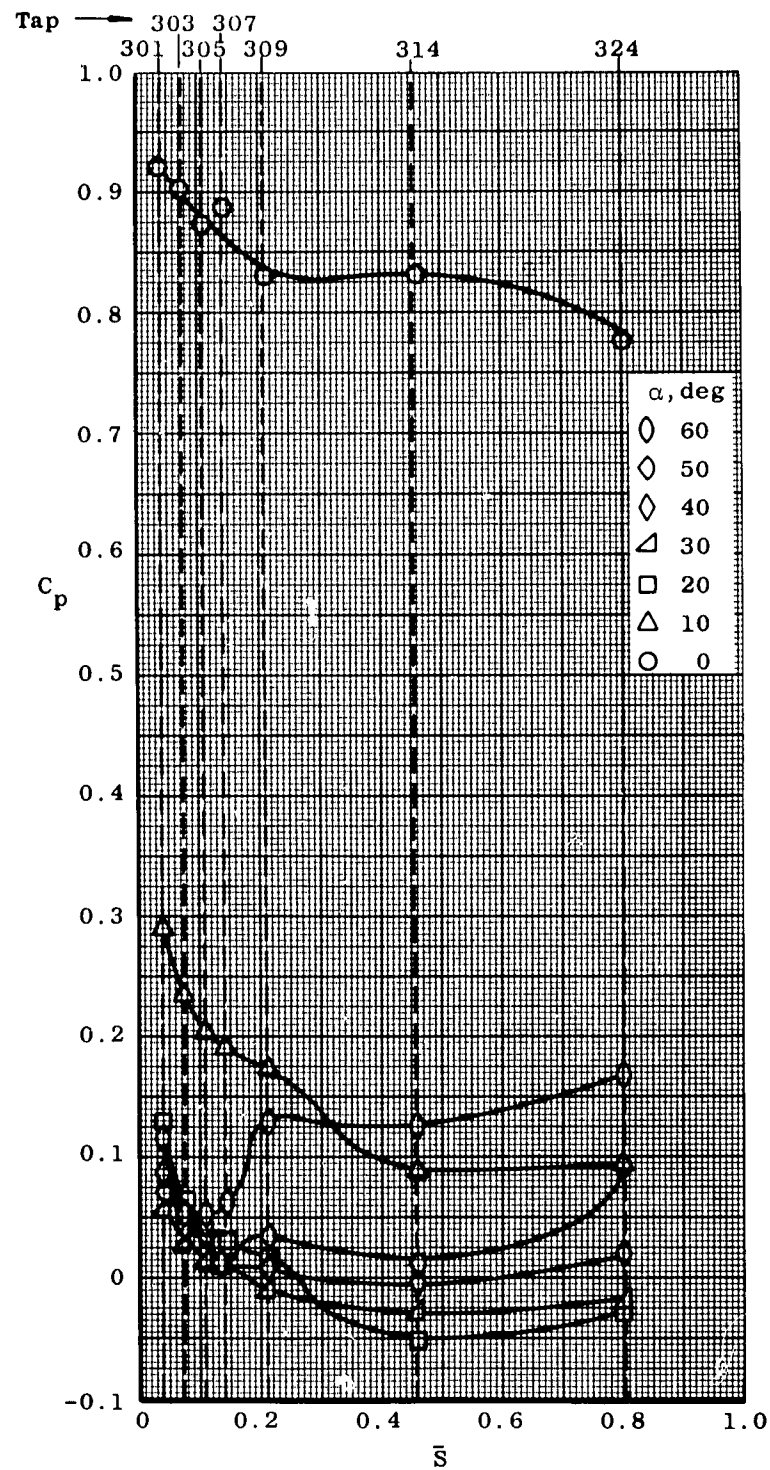


Fig. 7 Pressure Distribution along 180-deg Ray of Configuration 1

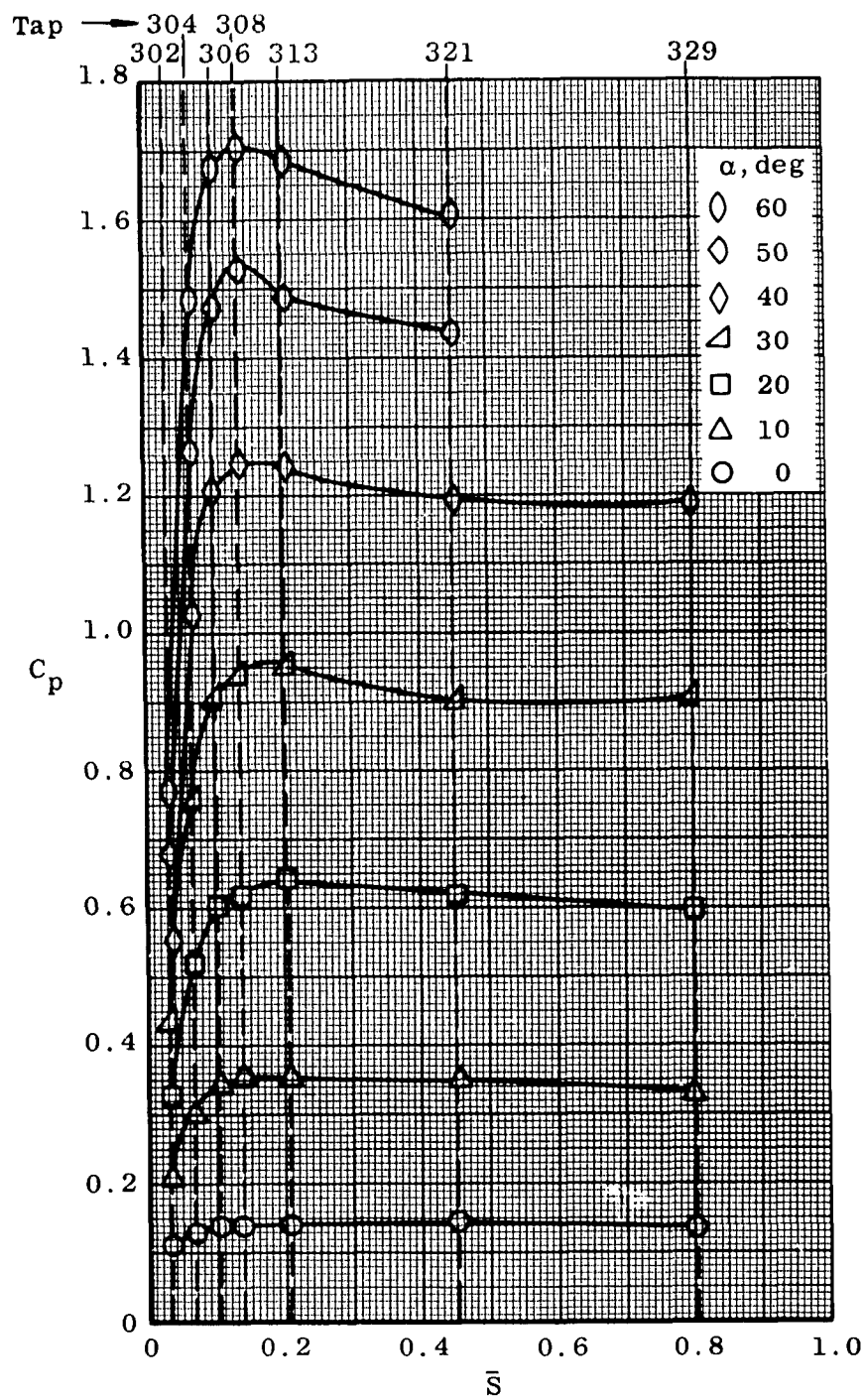


Fig. 8 Pressure Distribution along 100-deg Ray of Configuration 2

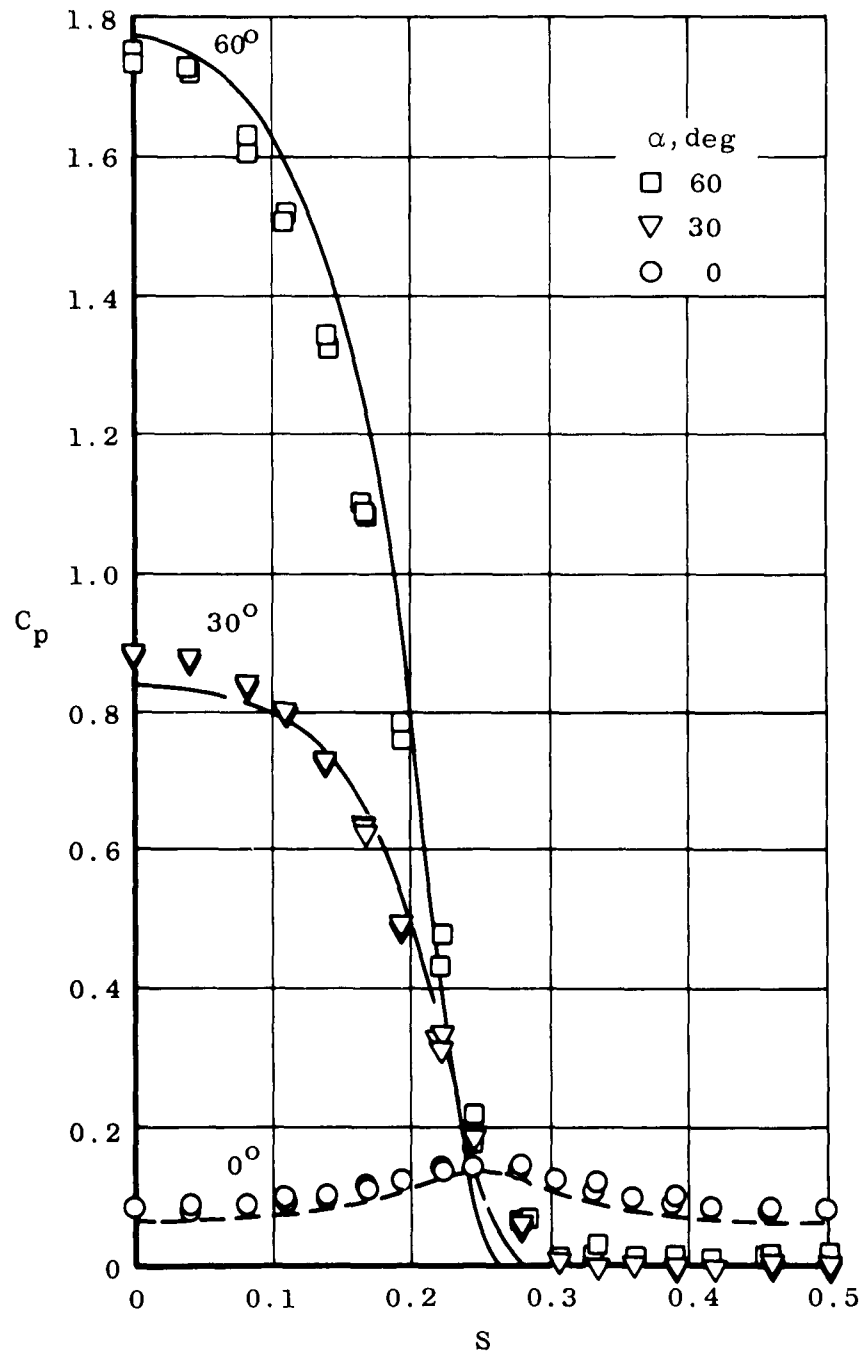


Fig. 9 Comparison between Measured Data and Newtonian Theory for Cross Sections 3.0, 6.5, and 11.5 of Configuration 1

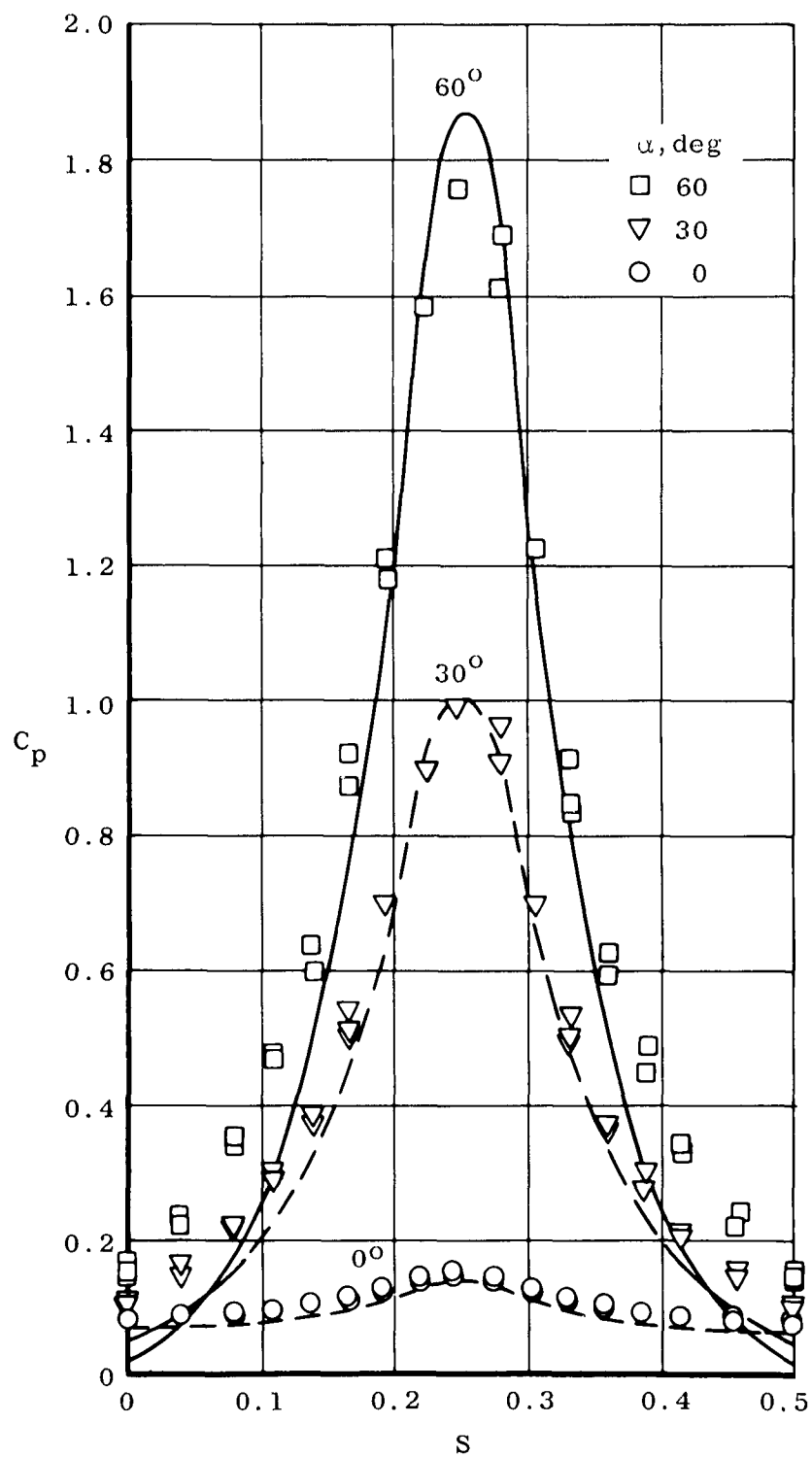


Fig. 10 Comparison between Measured Data and Newtonian Theory for Cross Sections 3.0, 6.5, and 11.5 of Configuration 2

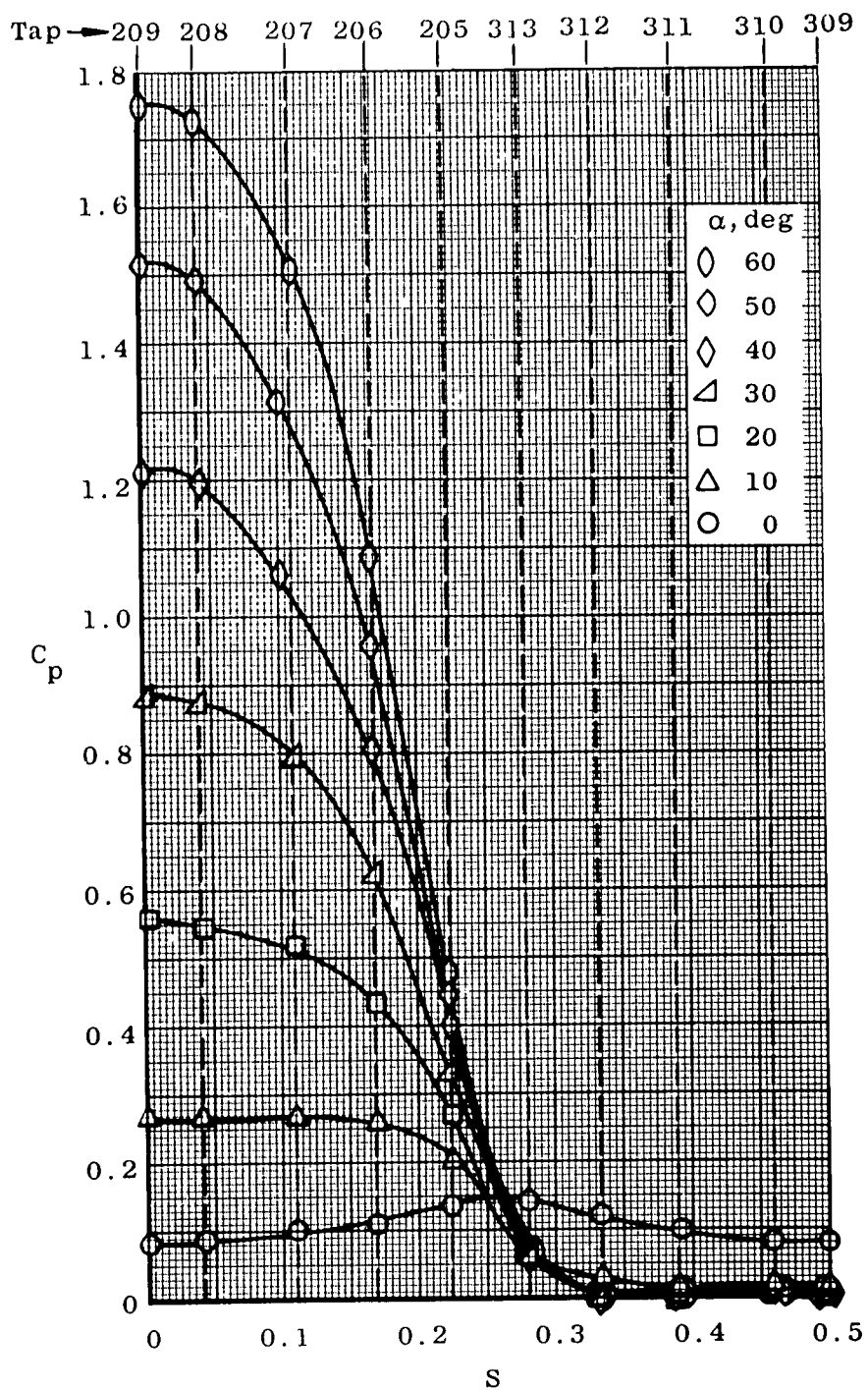


Fig. 11 Pressure Distribution for Cross Section 3.0 of Configuration 1

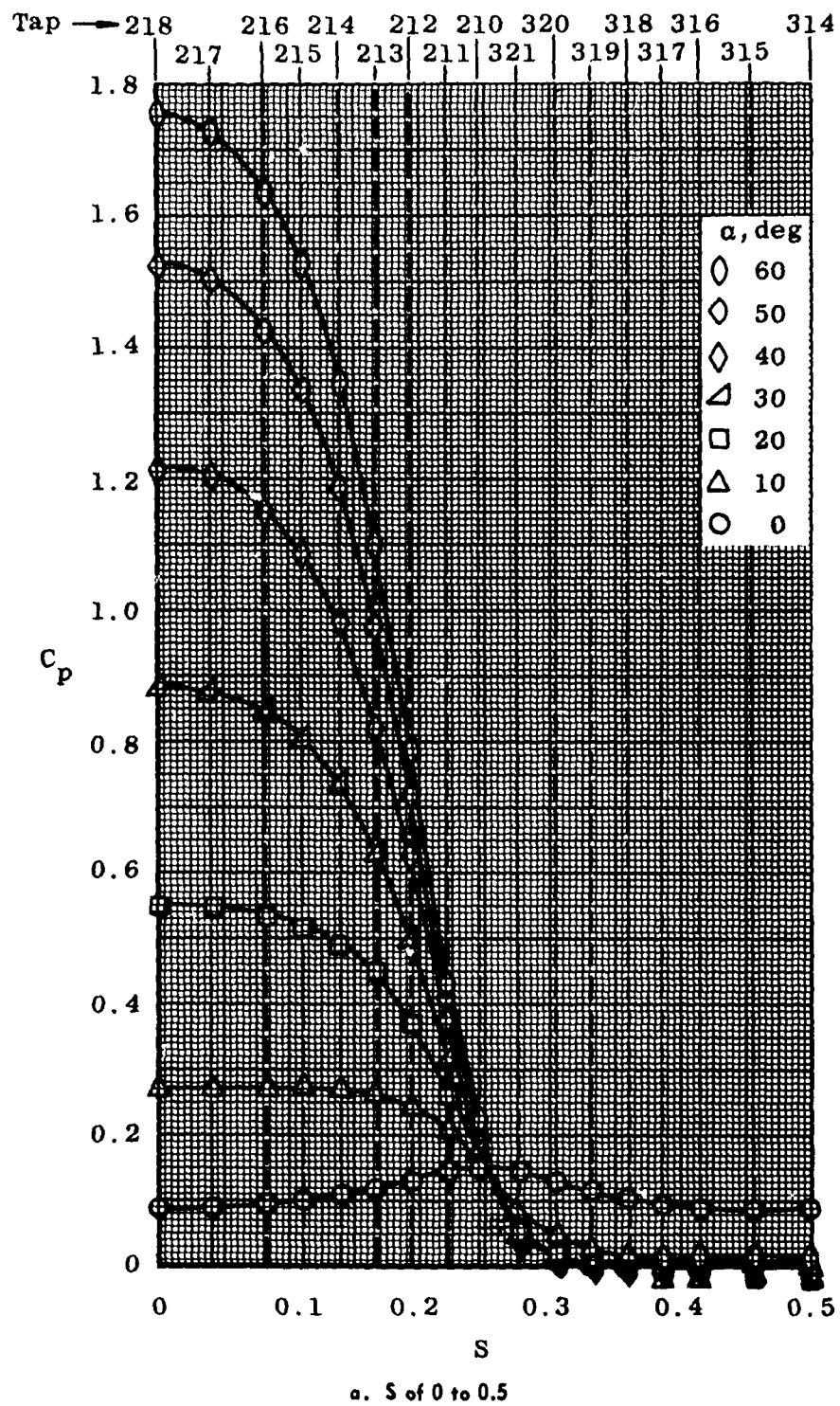


Fig. 12 Pressure Distribution for Cross Section 6.5 of Configuration 1

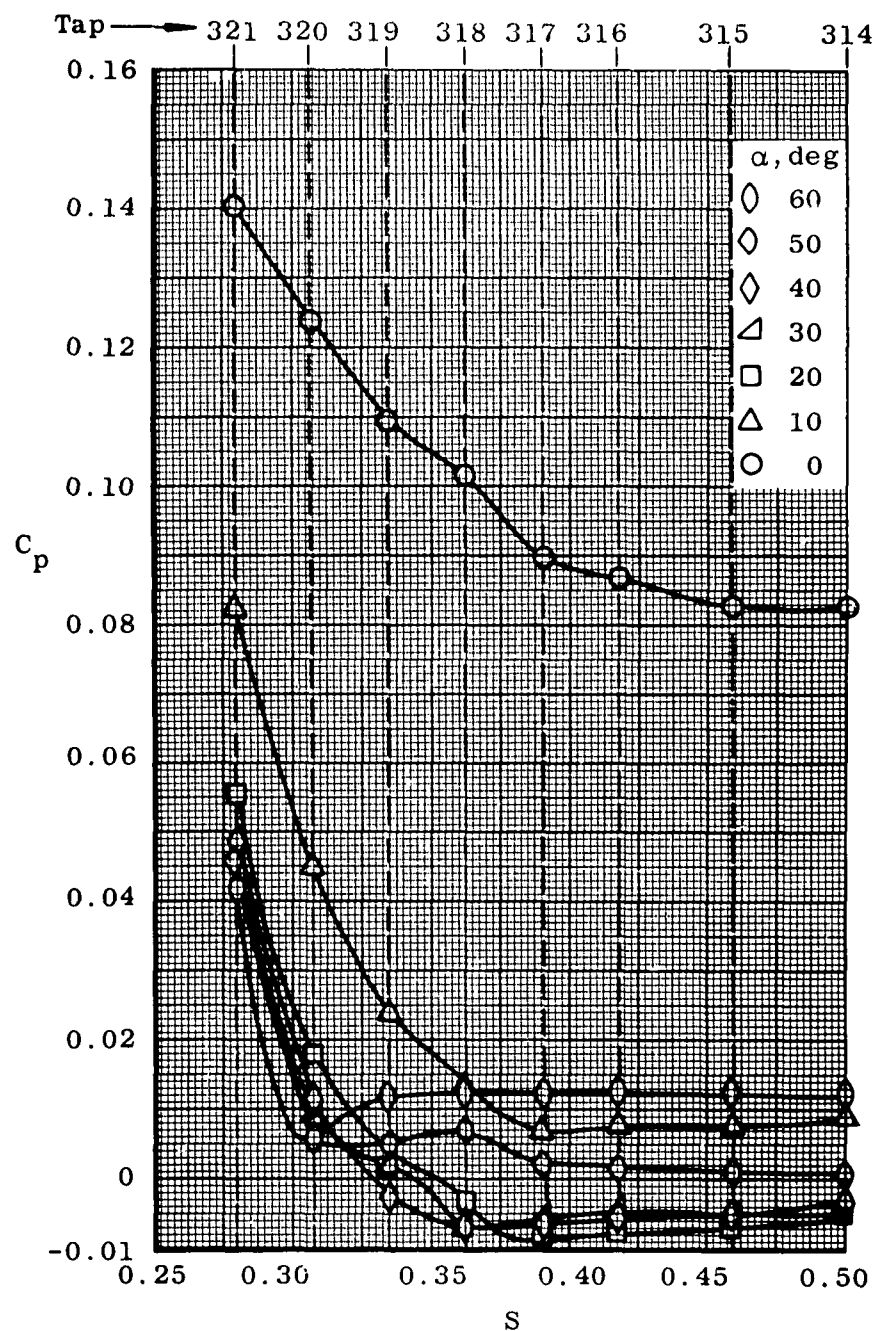
b. S of 0.25 to 0.5

Fig. 12 Concluded

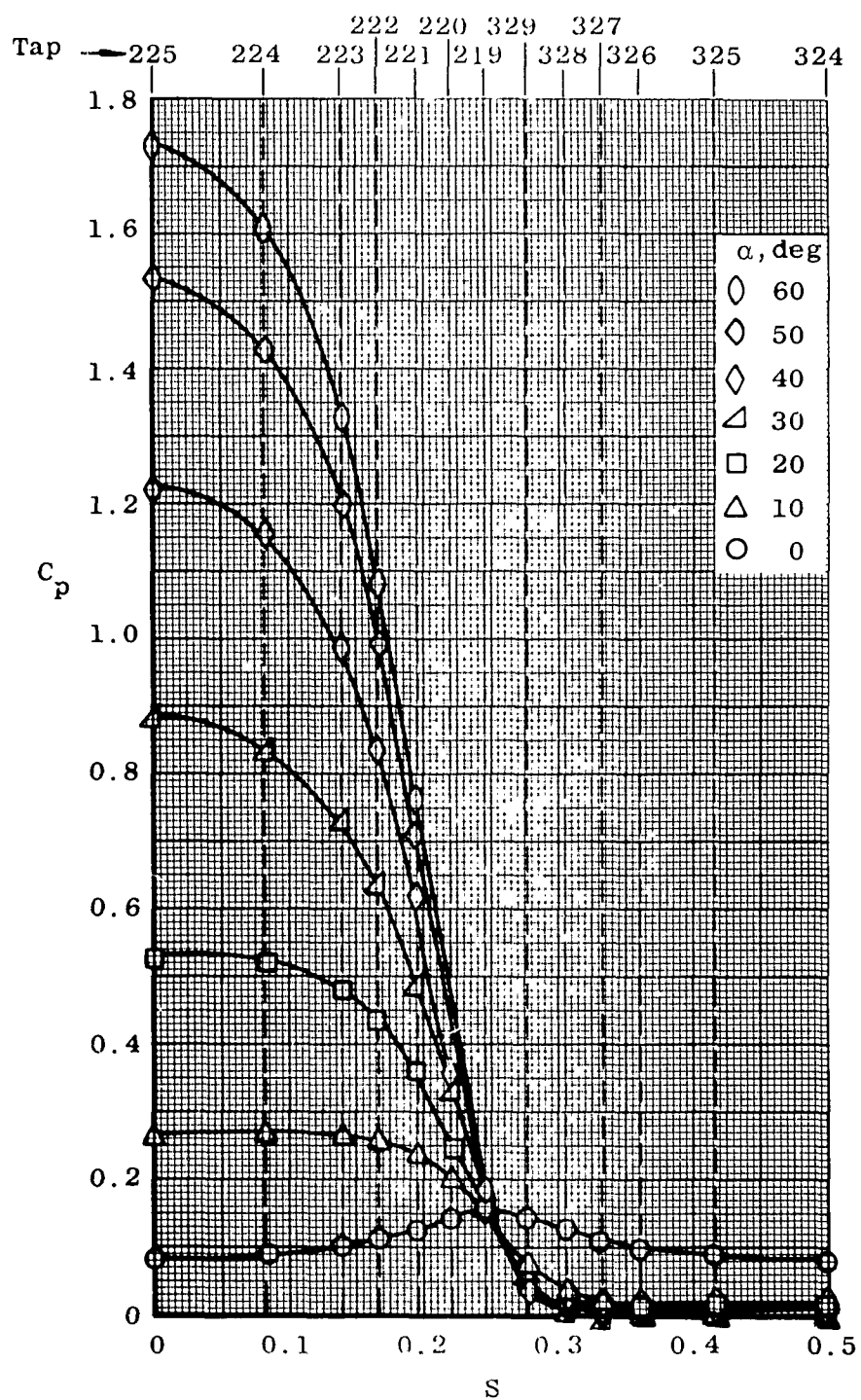


Fig. 13 Pressure Distribution for Cross Section 11.5 of Configuration 1

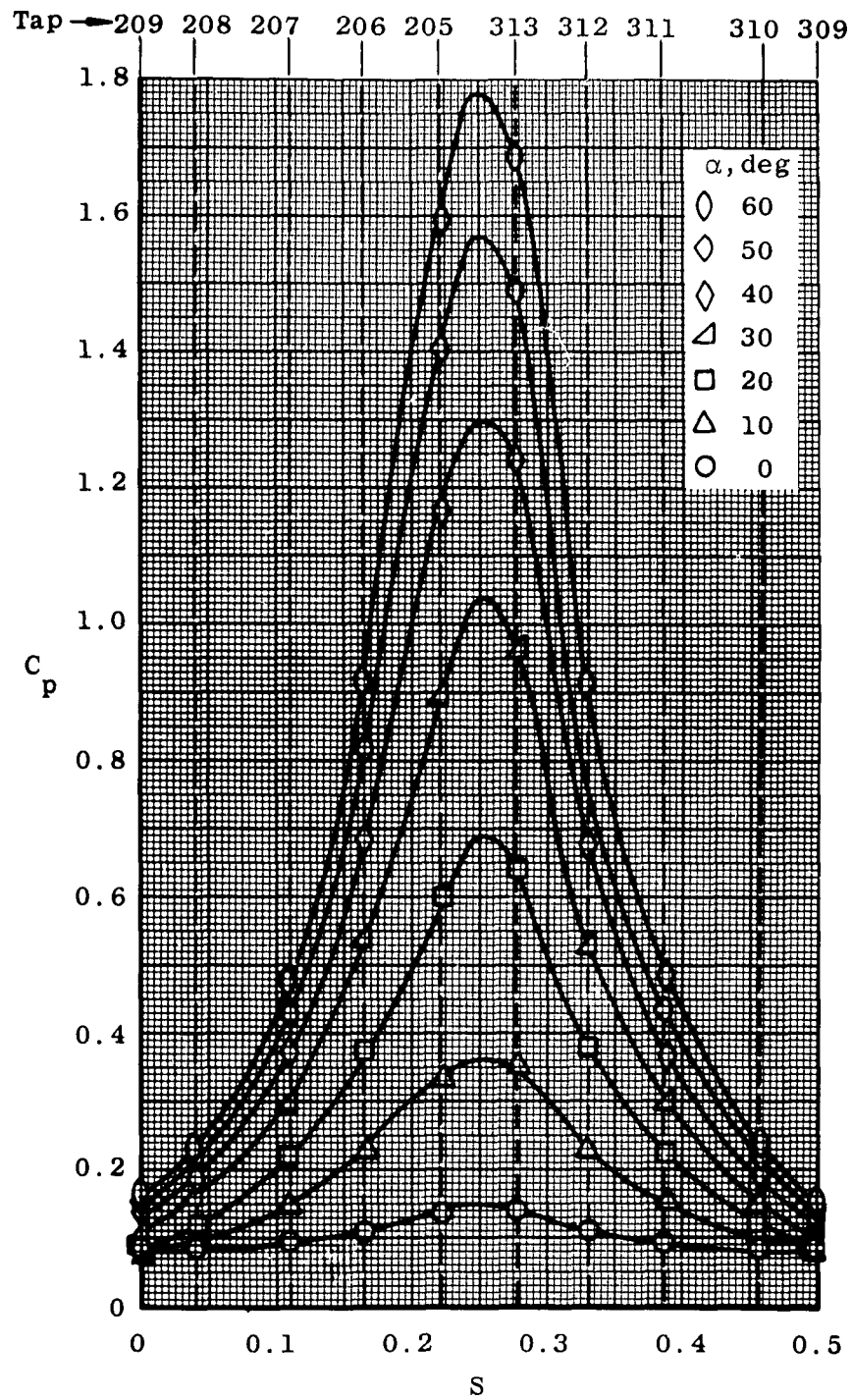


Fig. 14 Pressure Distribution for Cross Section 3.0 of Configuration 2

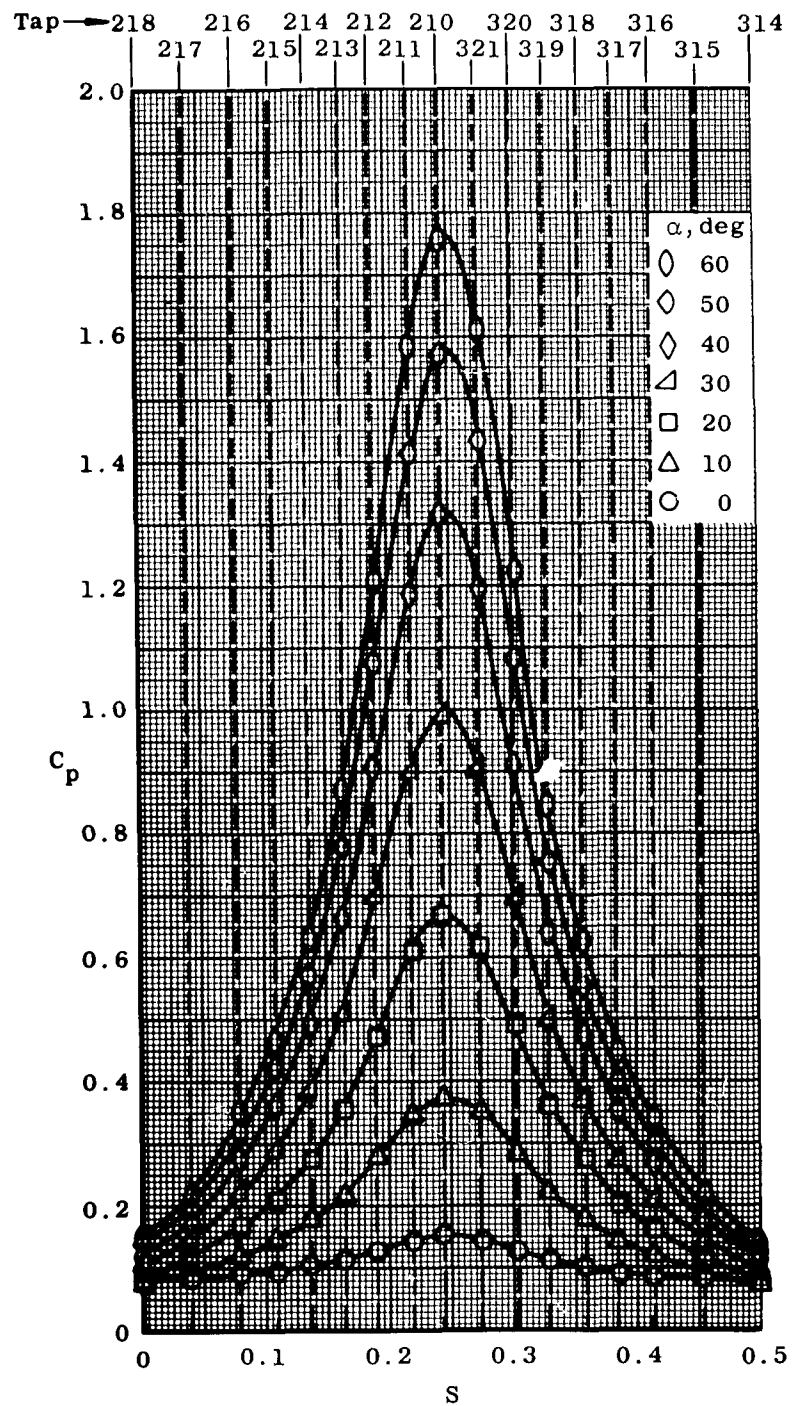


Fig. 15 Pressure Distribution for Cross Section 6.5 of Configuration 2

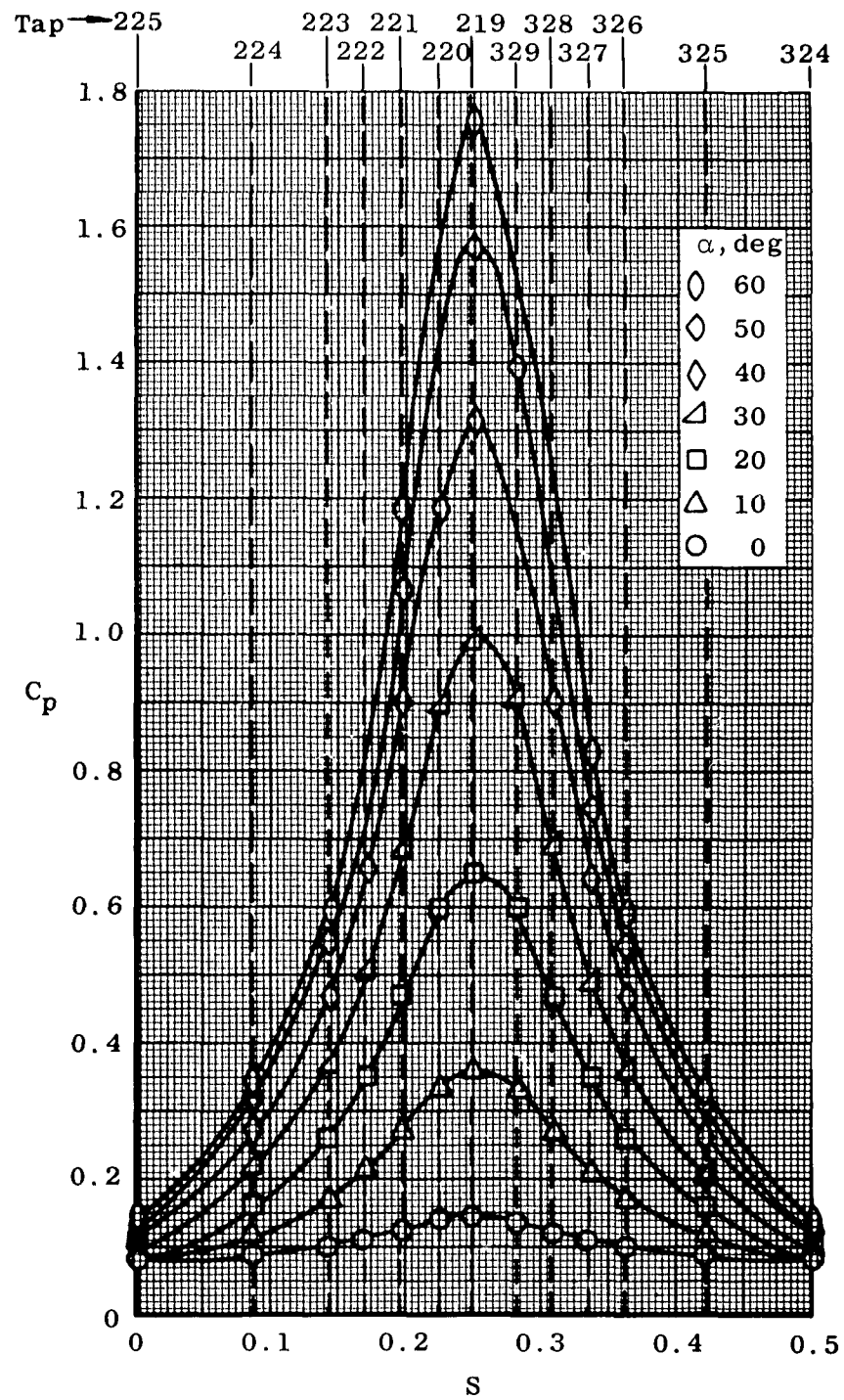


Fig. 16 Pressure Distribution for Cross Section 11.5 of Configuration 2

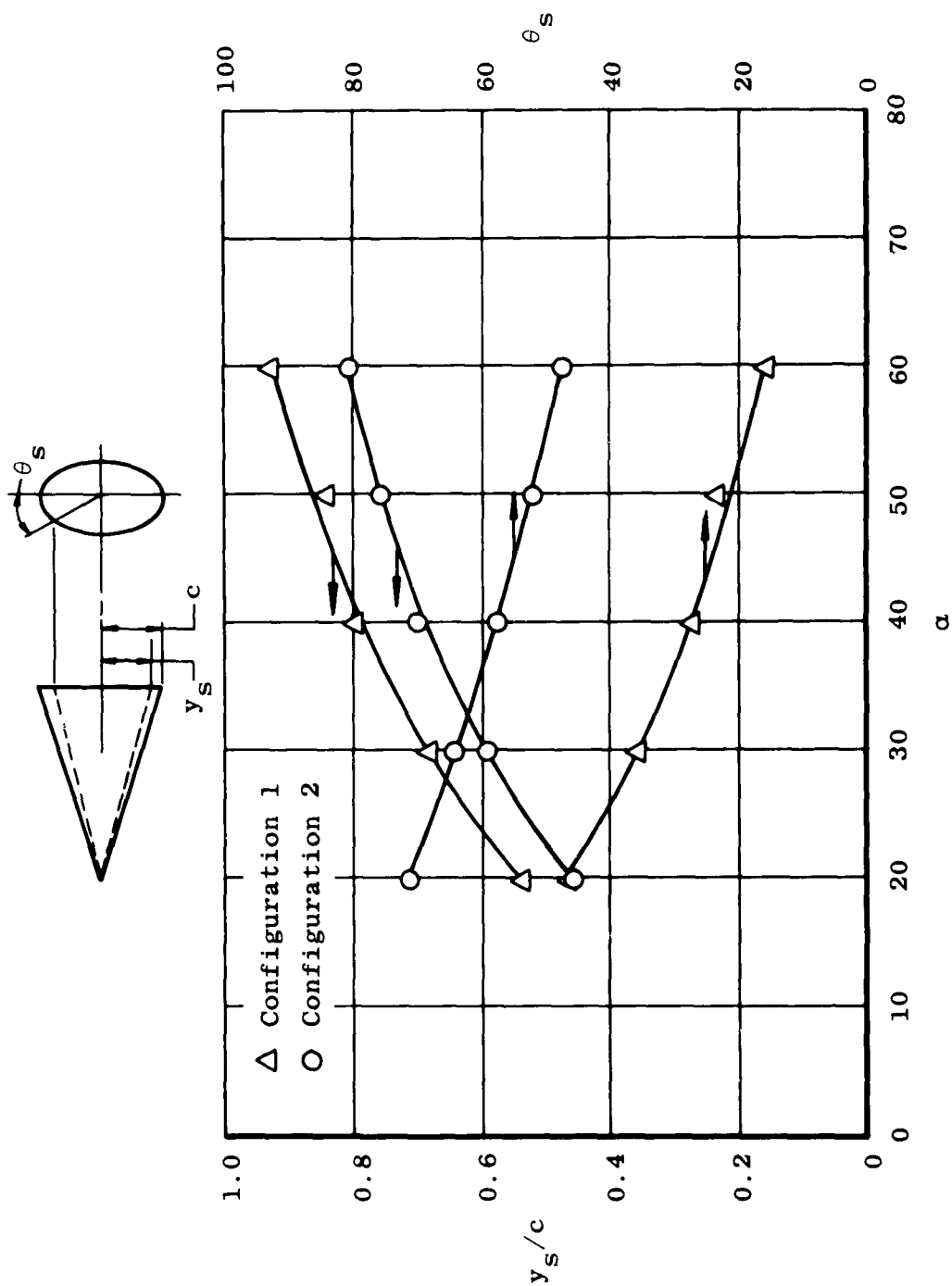
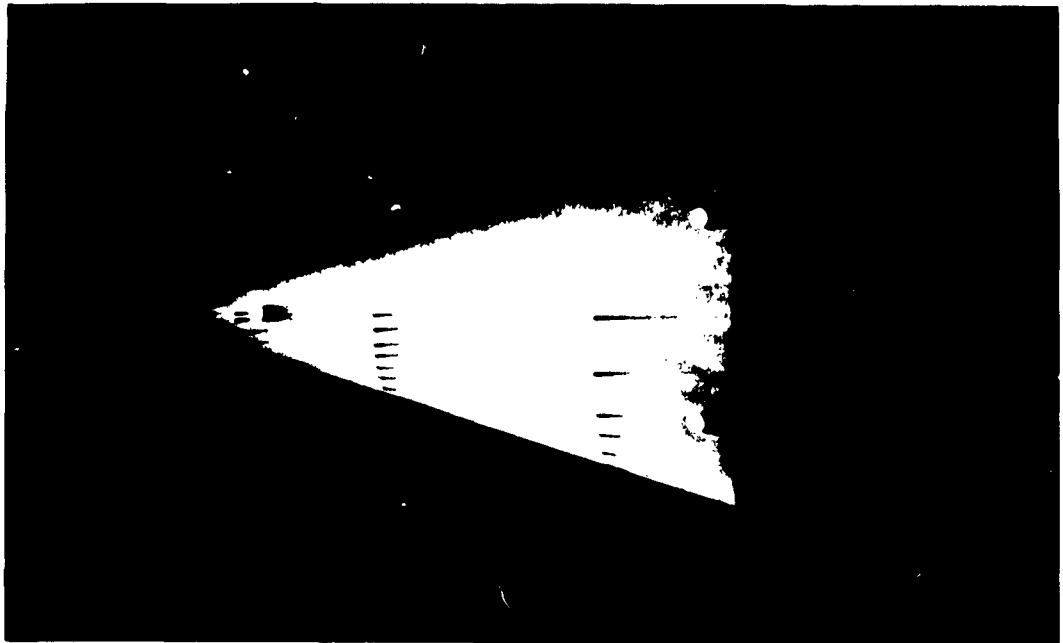
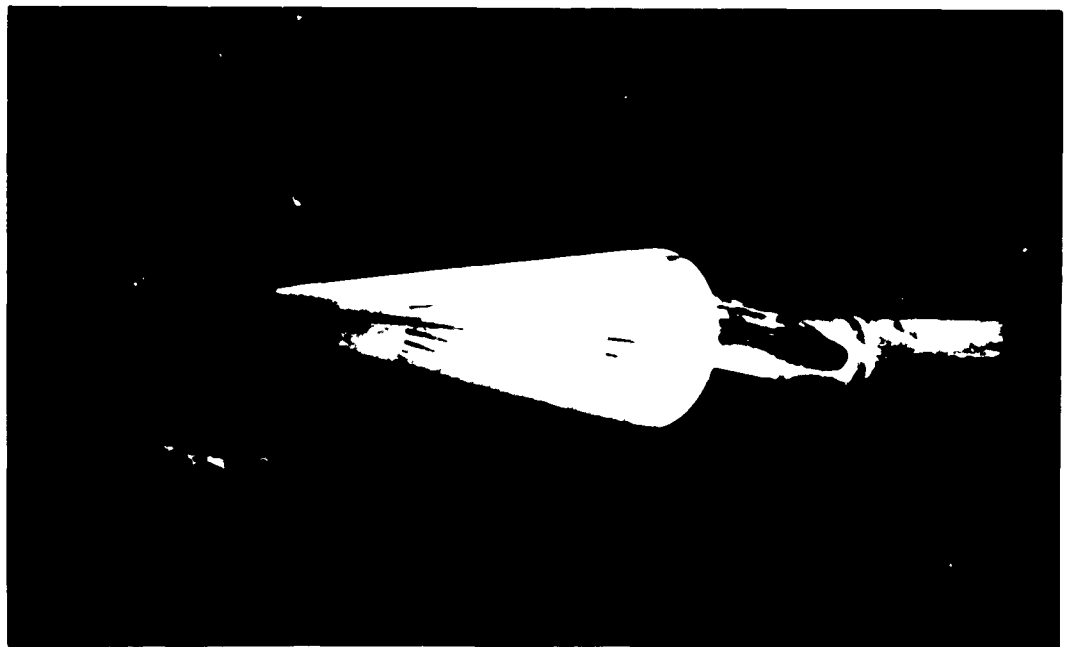


Fig. 17 Effect of Angle of Attack on Point of Flow Separation



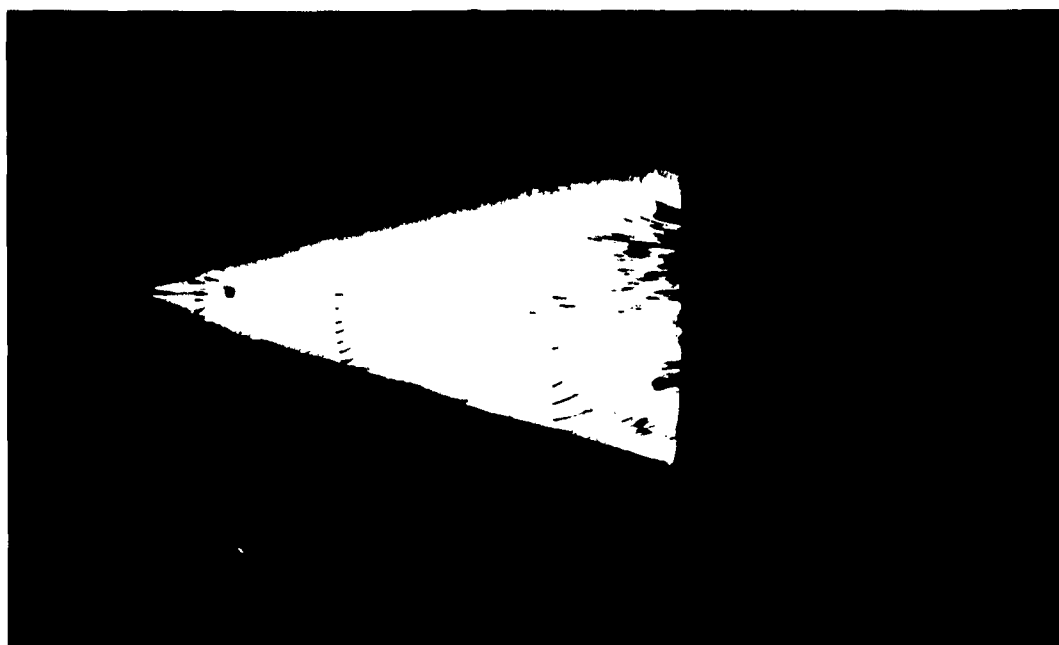
Top View



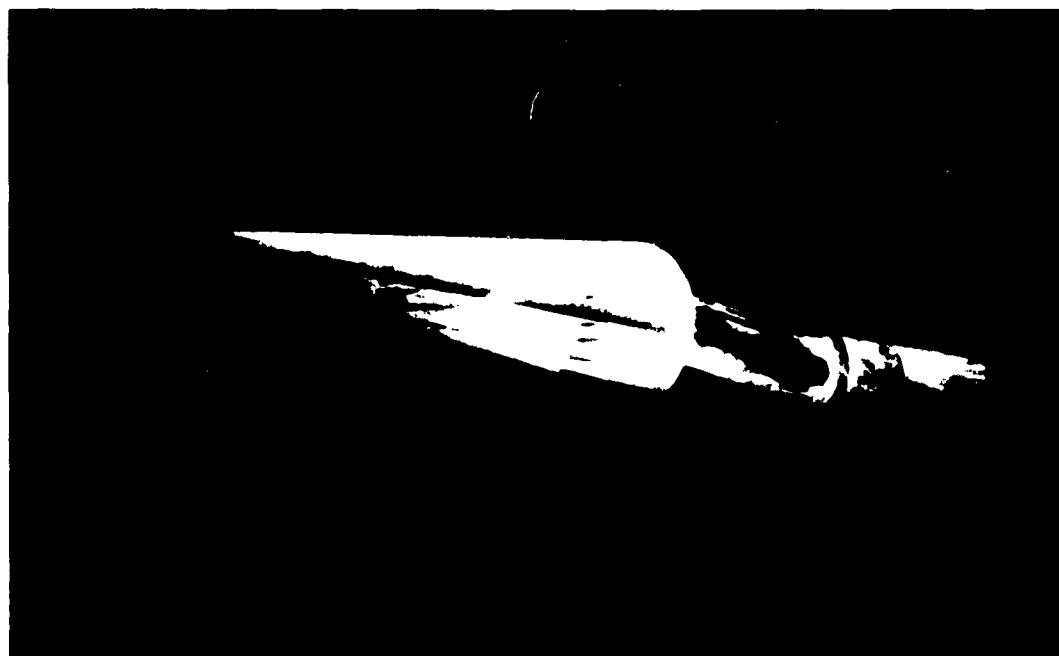
Side View

$\alpha = 0 \text{ deg}$

Fig. 18 Oil Flow Photographs of Configuration 1



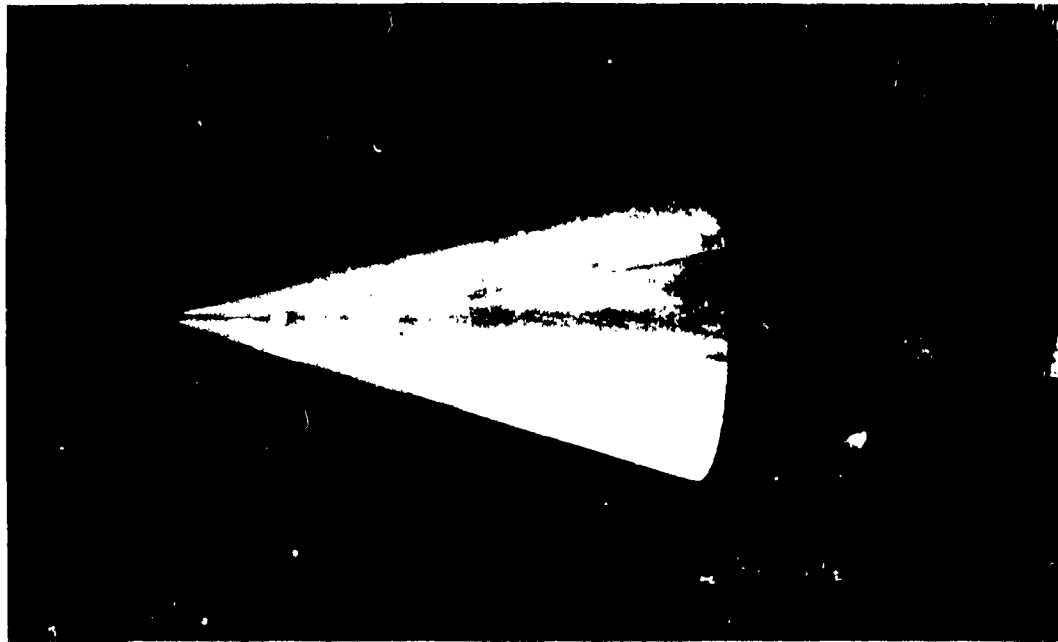
Top View



Side View

b. $\alpha = 10$ deg

Fig. 18 Continued



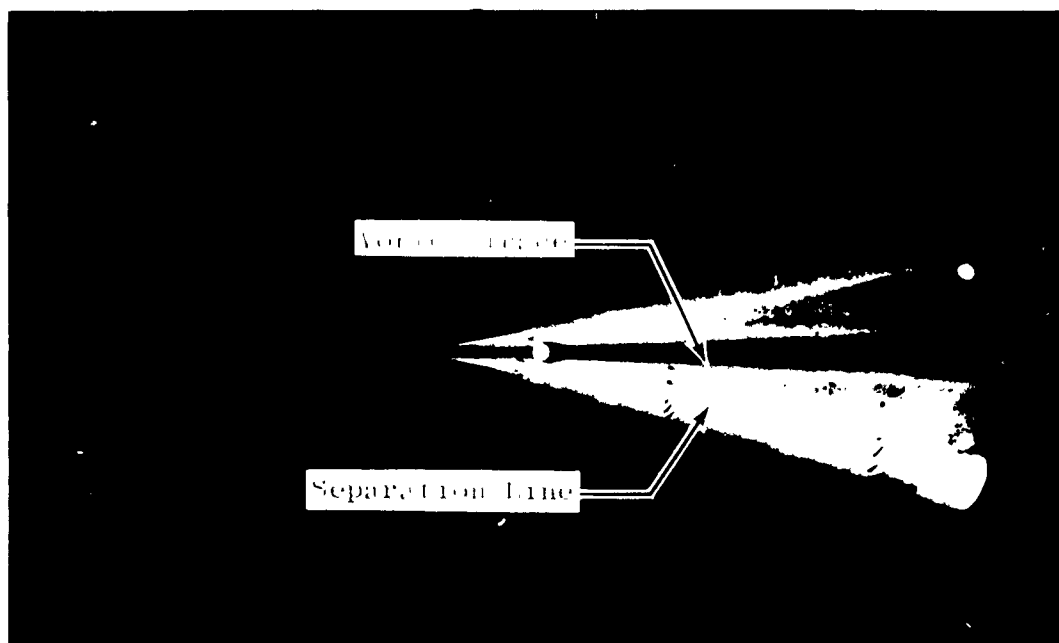
Top View



Side View

c. $\alpha = 20$ deg

Fig. 18 Continued



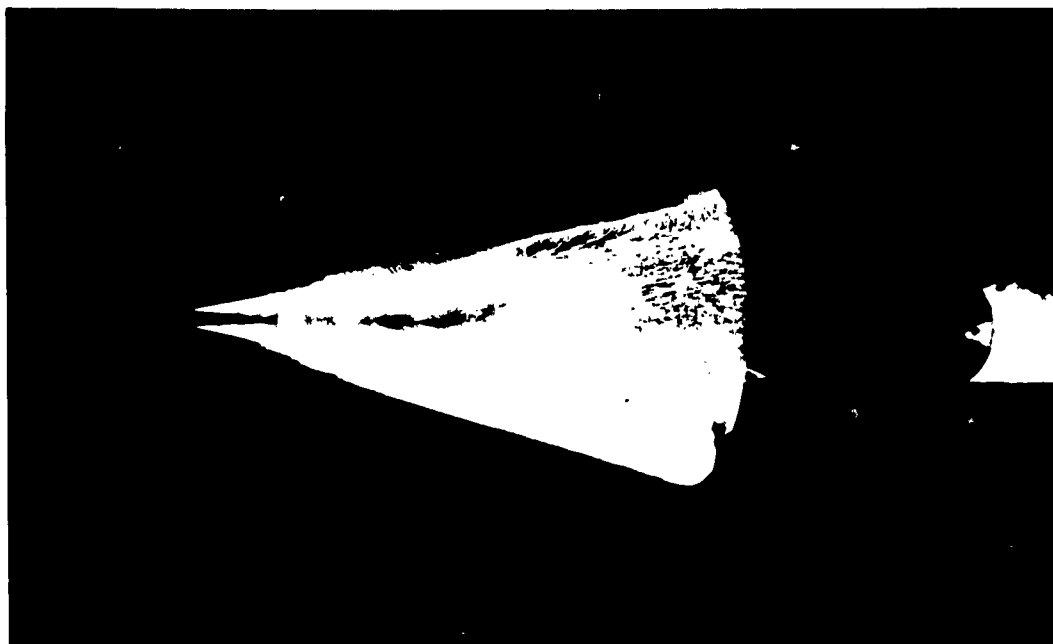
Top View



Side View

d. $\alpha = 30$ deg

Fig. 18 Continued



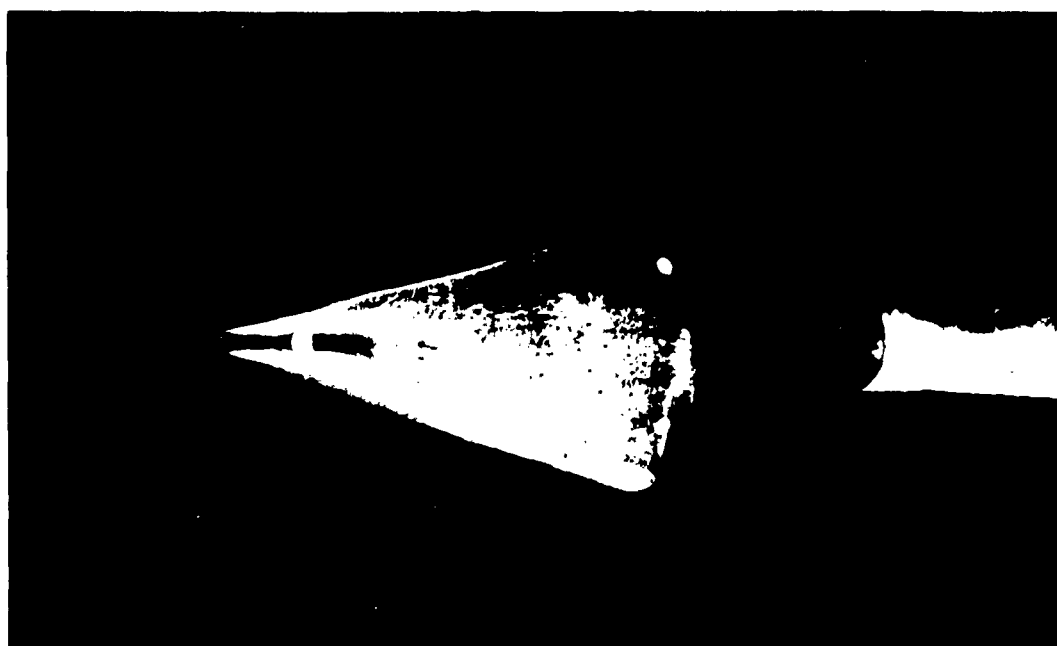
Top View



Side View

e. $\alpha = 40$ deg

Fig. 18 Continued



Top View



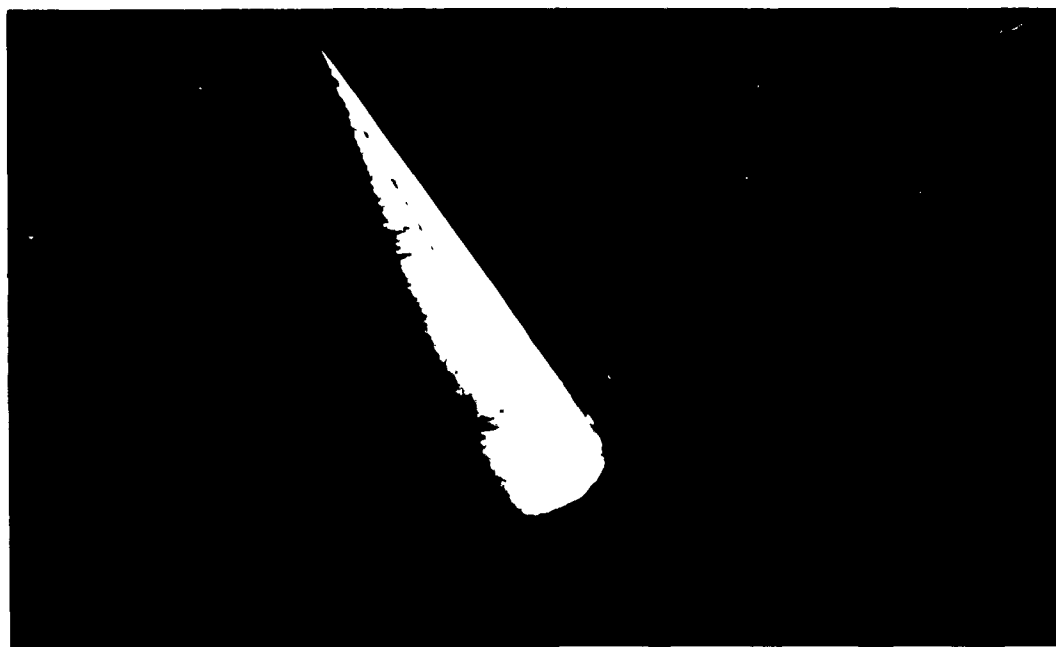
Side View

f. $\alpha = 50$ deg

Fig. 18 Continued



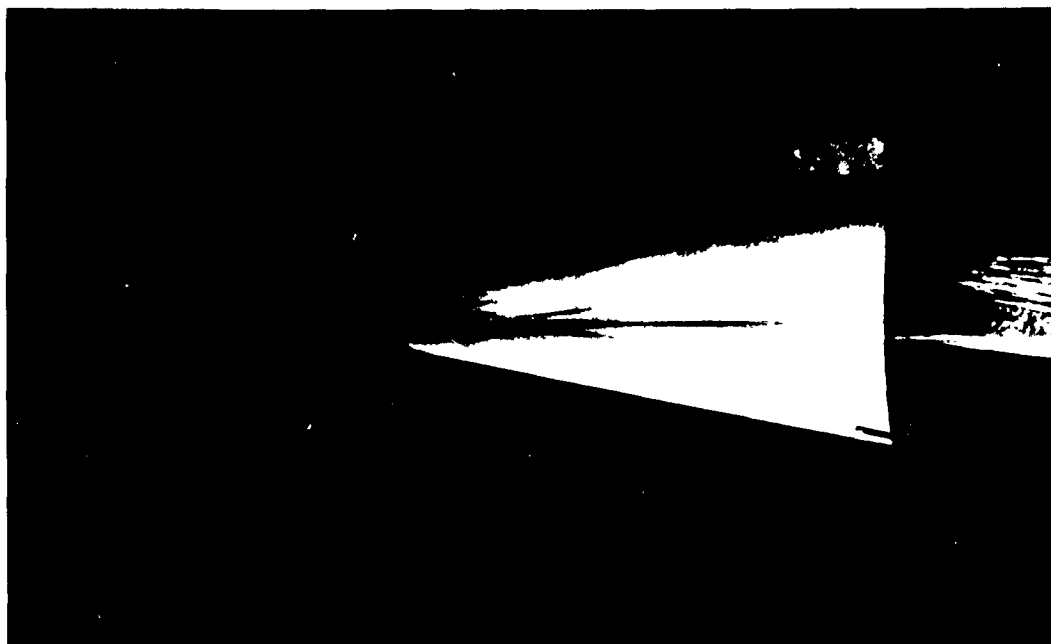
Top View



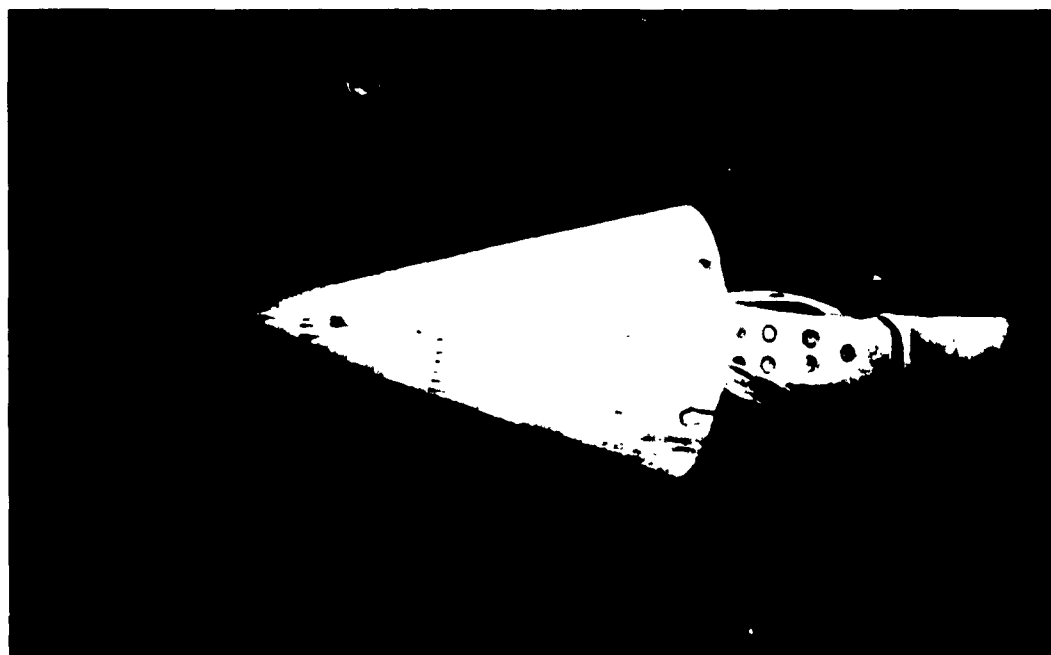
Side View

g. $\alpha = 60$ deg

Fig. 18 Concluded

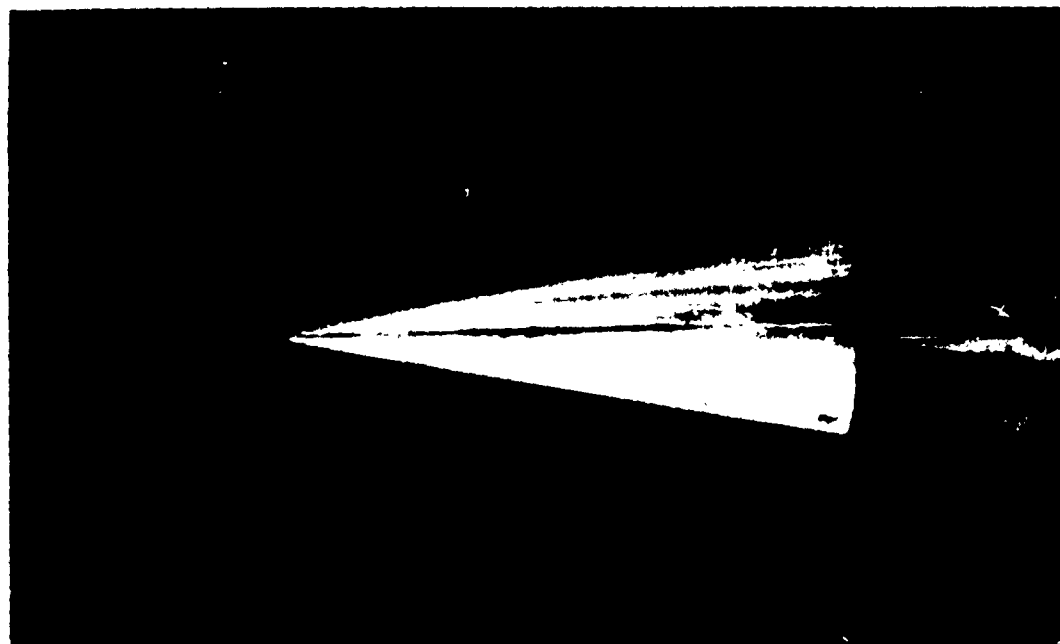


Top View

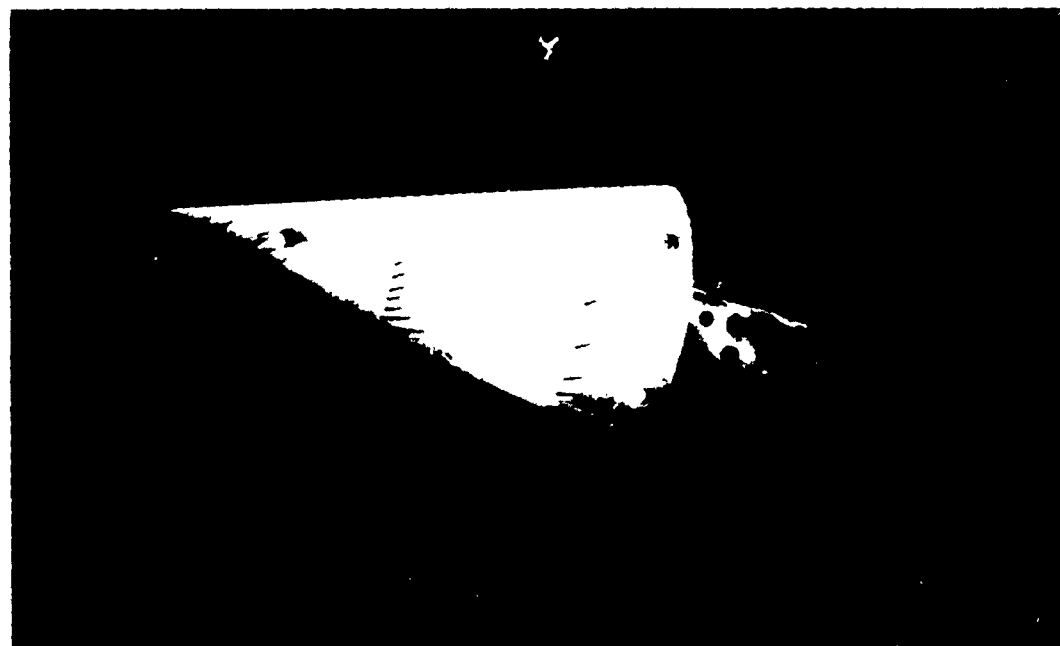


Side View
a. $\alpha = 0$ deg

Fig. 19 Oil Flow Photographs of Configuration 2



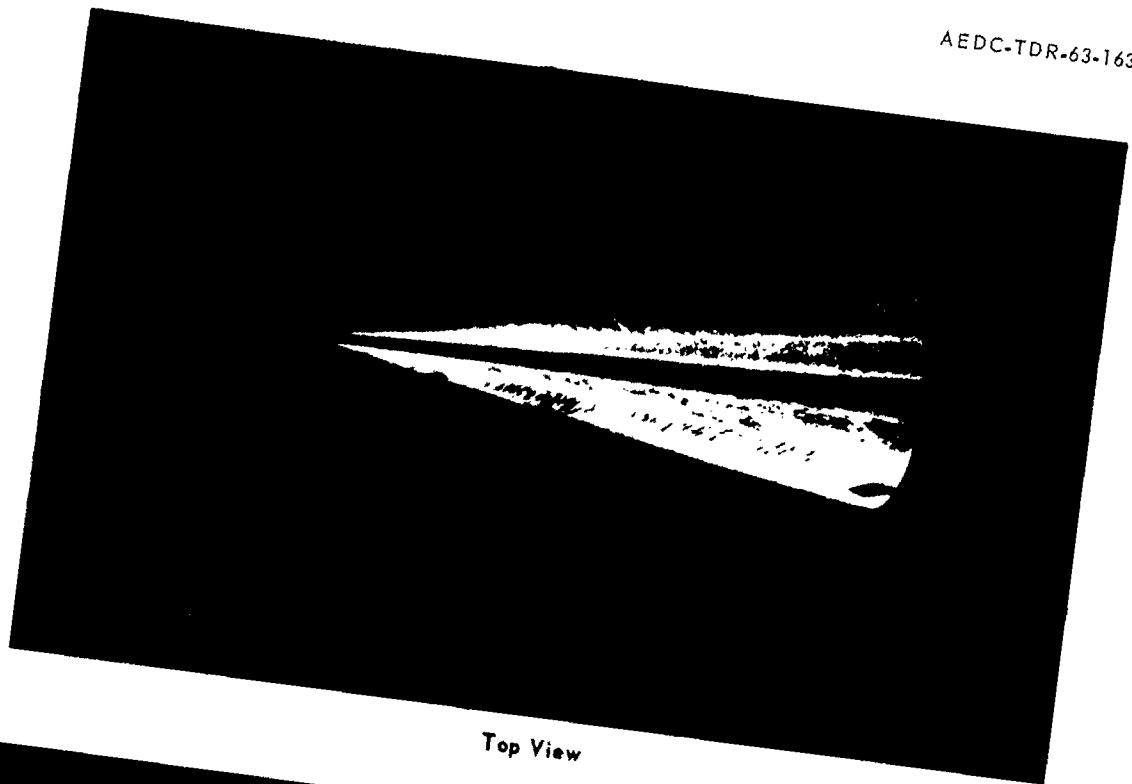
Top View



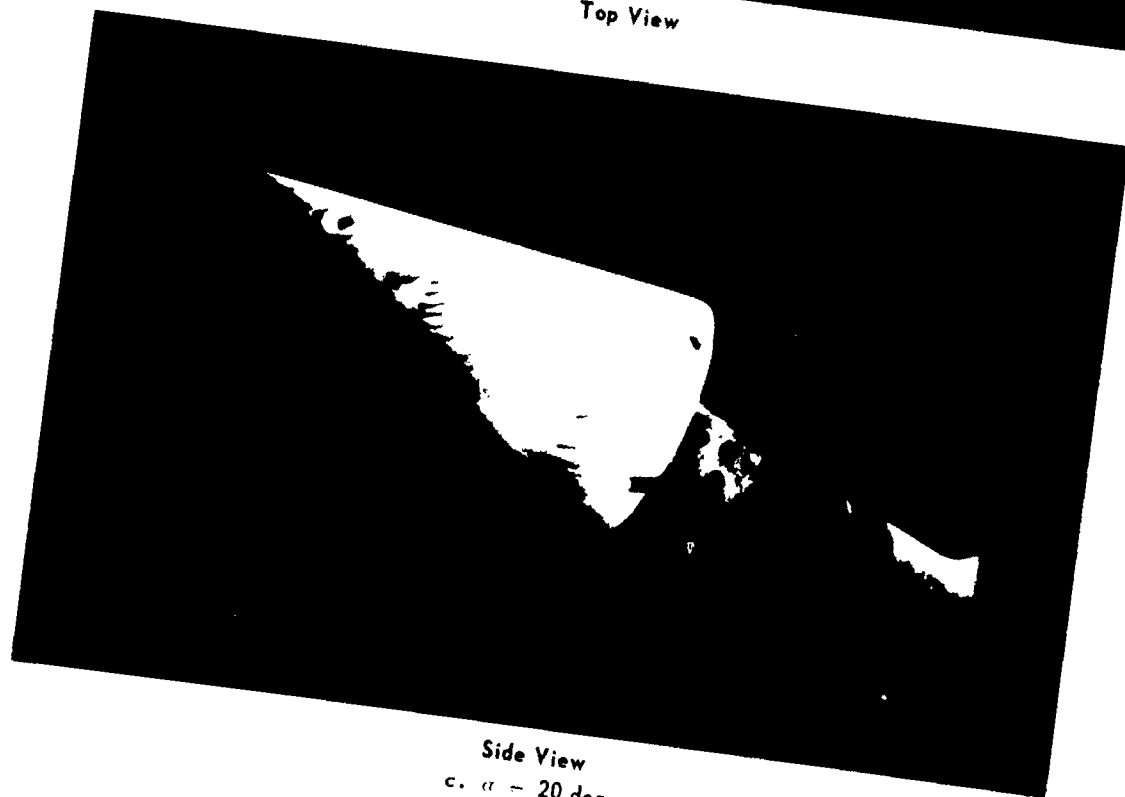
Side View

b. $\alpha \sim 10$ deg

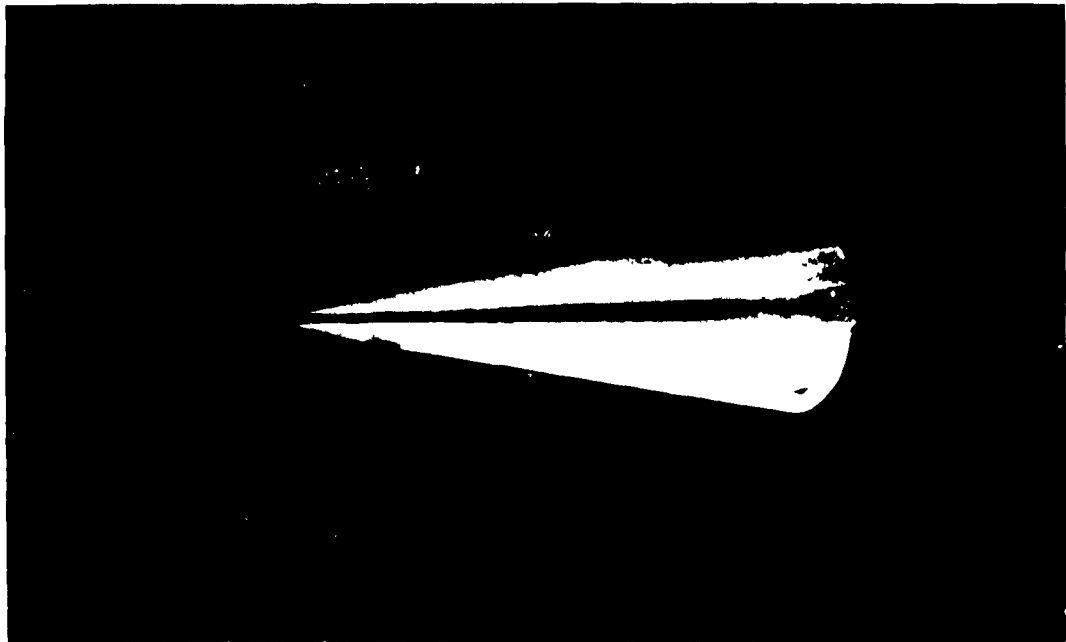
Fig. 19 Continued



Top View



Side View
c. $\alpha = 20$ deg
Fig. 19 Continued



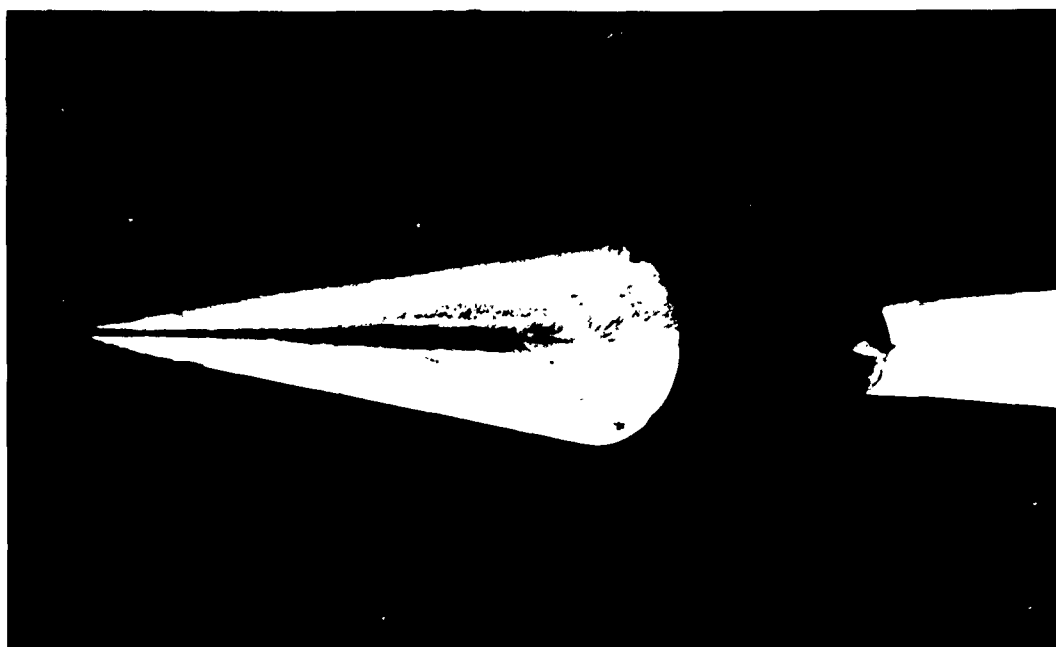
Top View



Side View

d. $\alpha = 30$ deg

Fig. 19 Continued



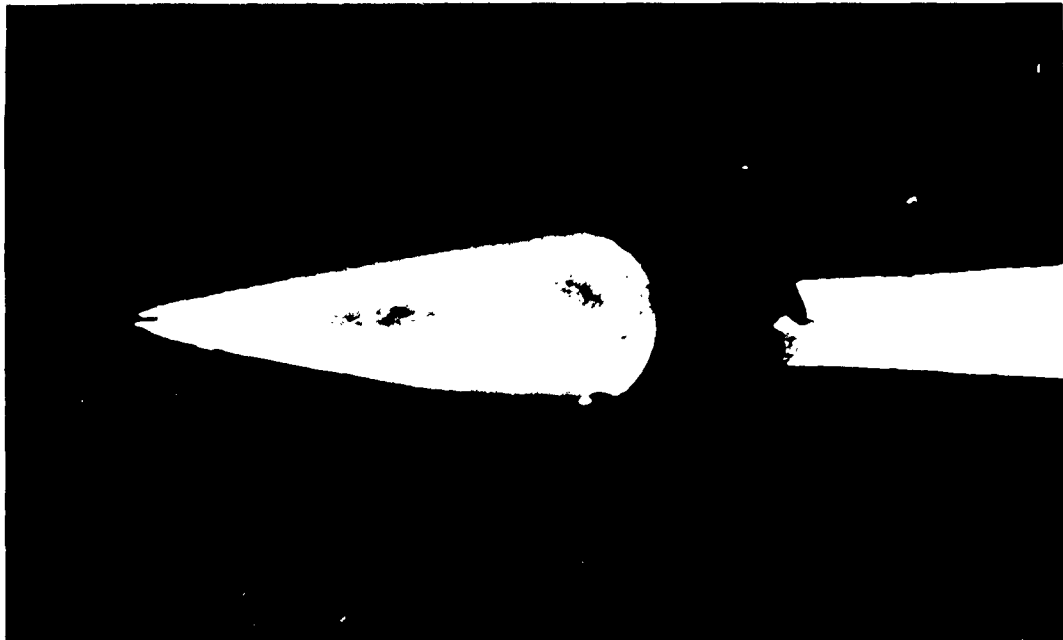
Top View



Side View

e. $\alpha = 40$ deg

Fig. 19 Continued



Top View



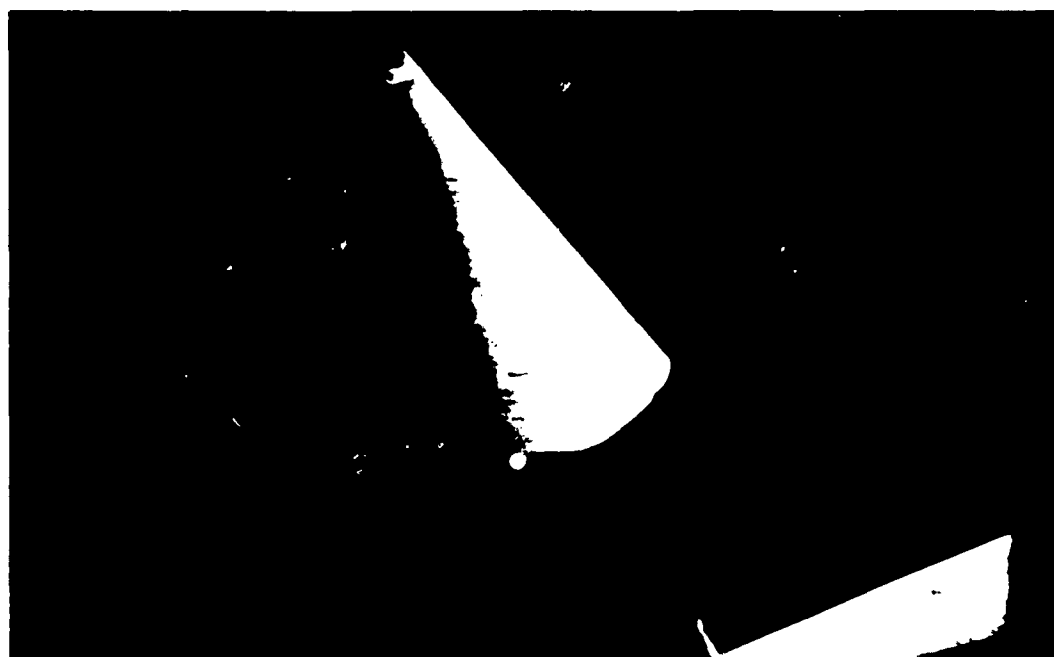
Side View

f. $\alpha = 50$ deg

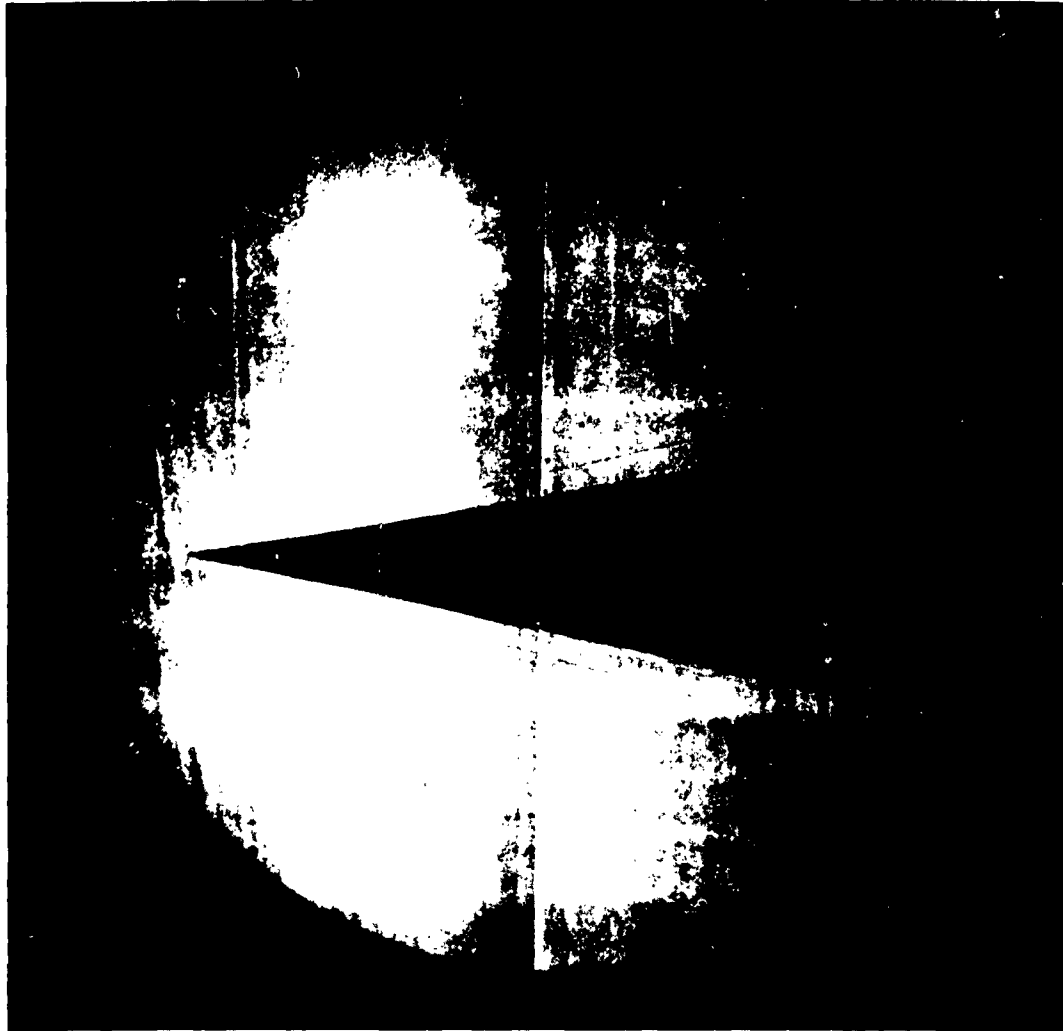
Fig. 19 Continued



Top View

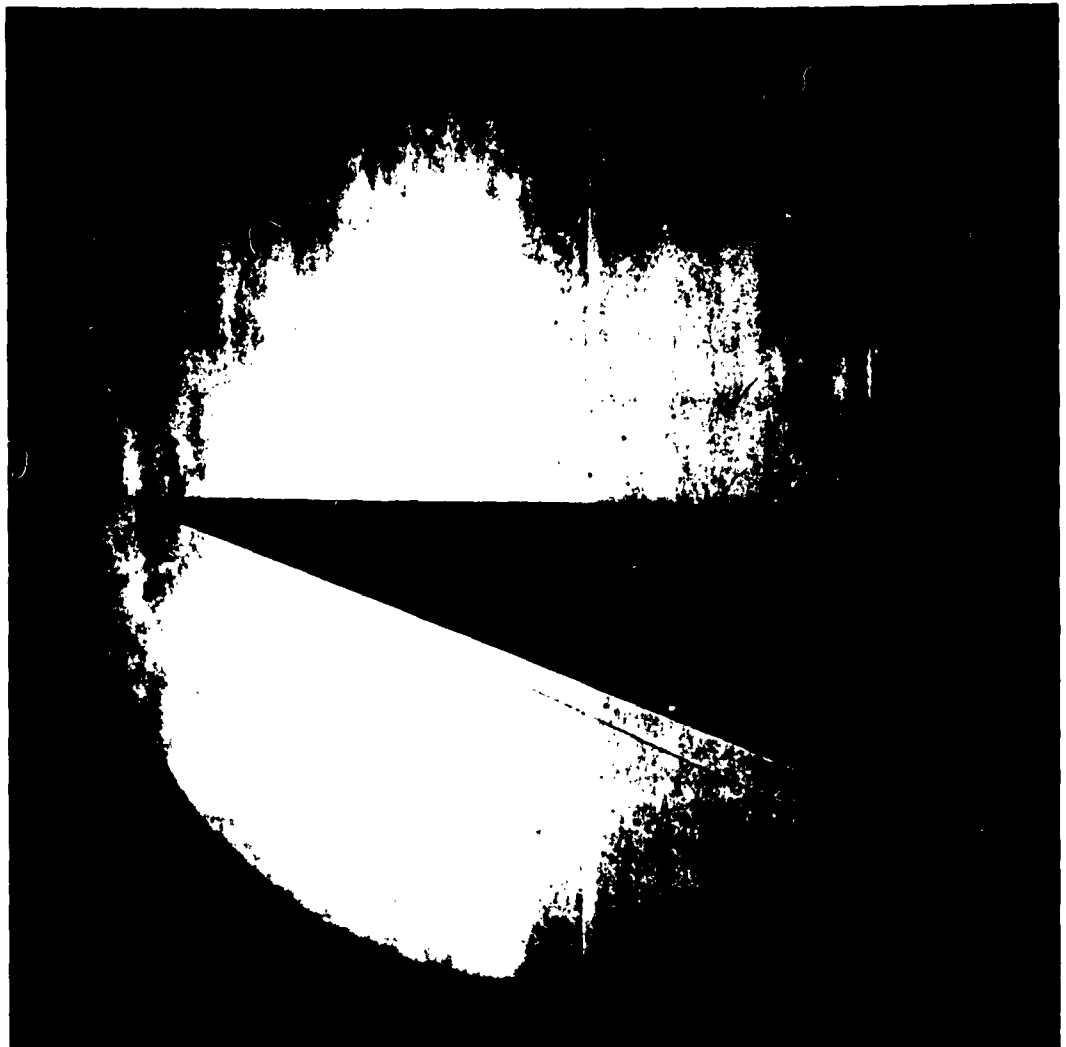


Side View
g. $\alpha = 60$ deg
Fig. 19 Concluded

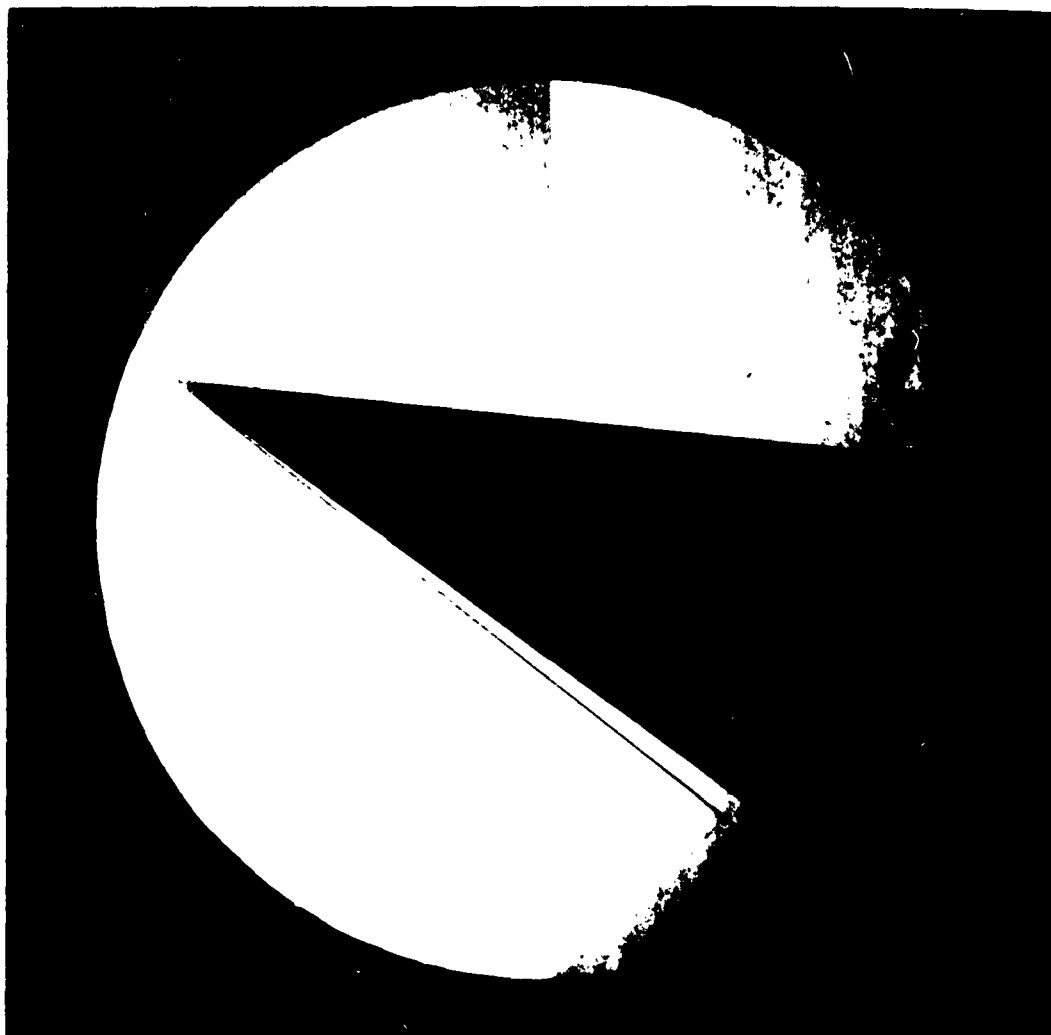


a. $\alpha = 0 \text{ deg}$

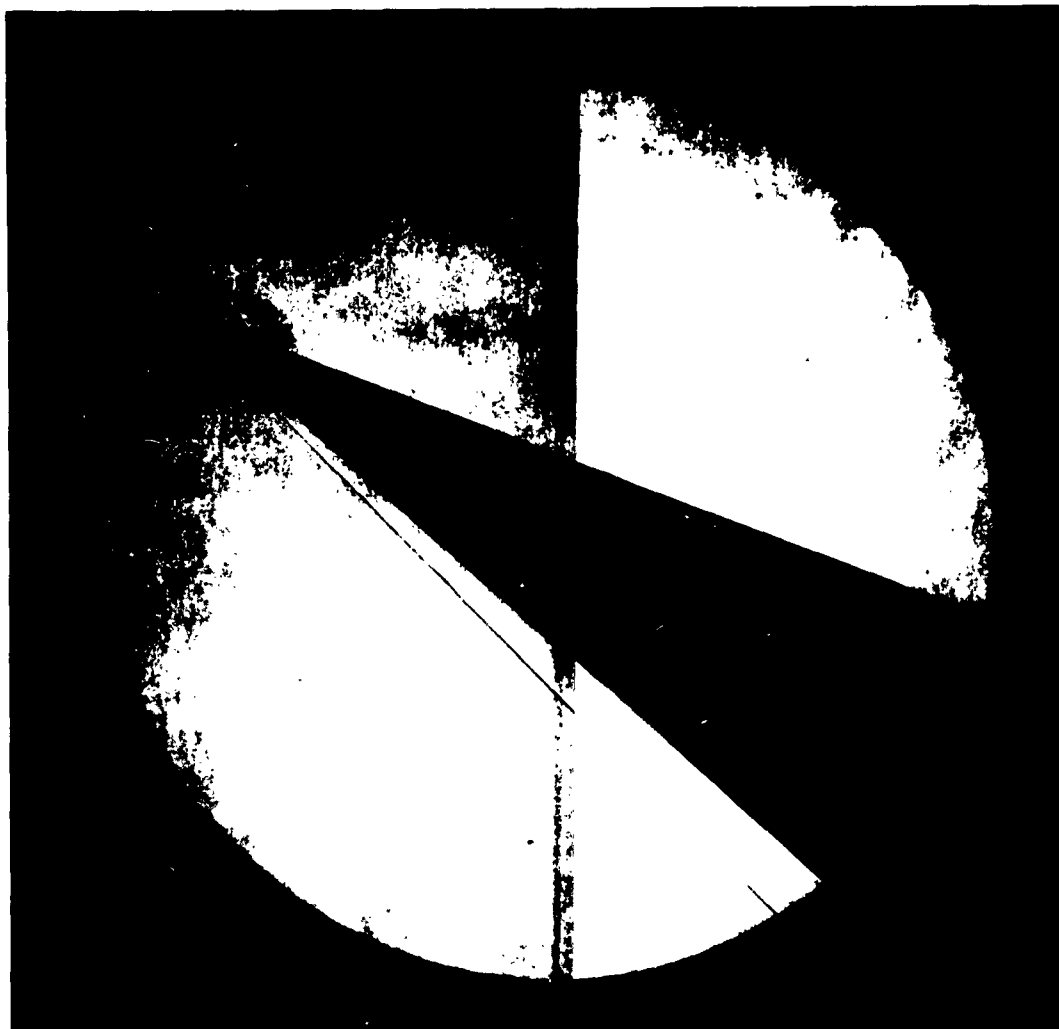
Fig. 20 Shadowgraphs of Configuration 1



b. $\alpha \approx 10$ deg
Fig. 20 Continued



c. $\alpha = 20$ deg
Fig. 20 Continued



d. $\alpha = 30 \text{ deg}$

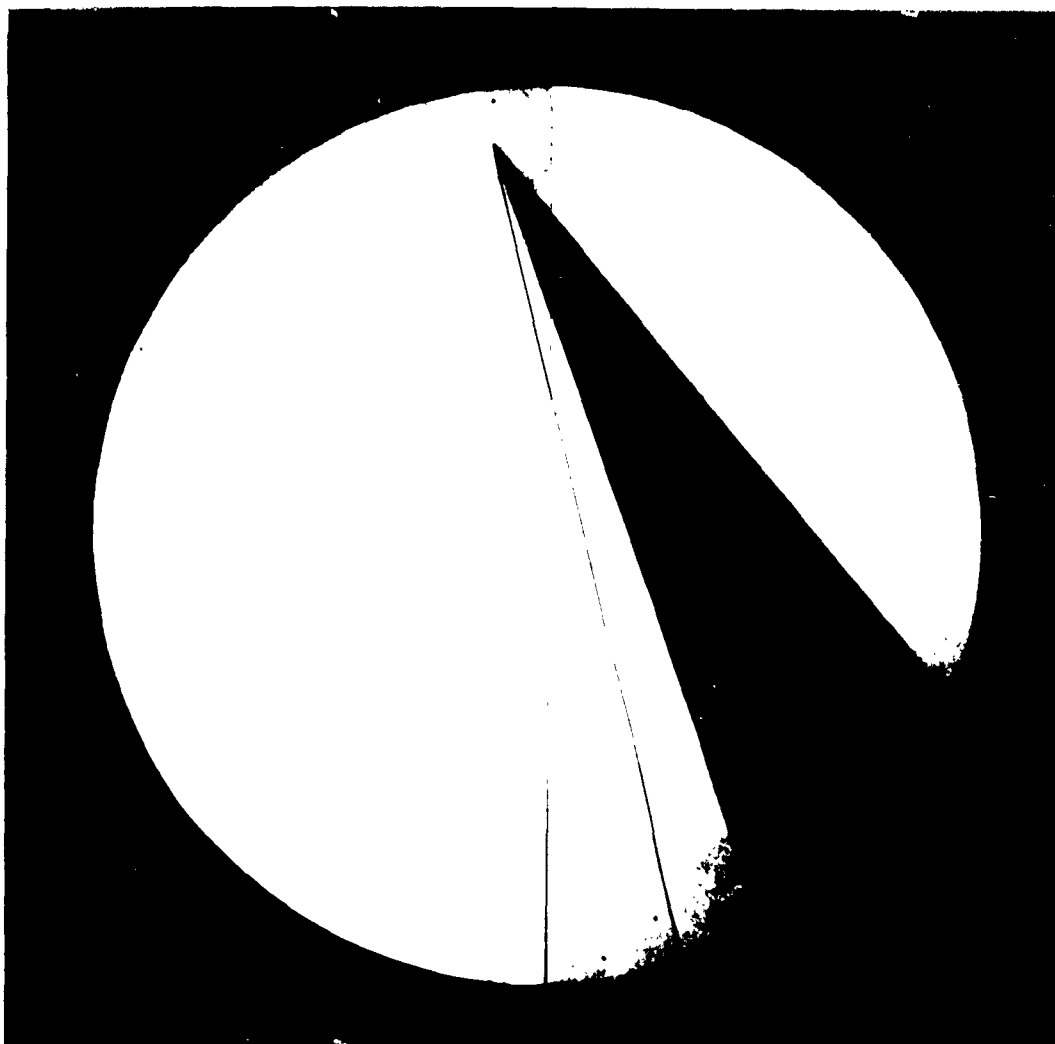
Fig. 20 Continued



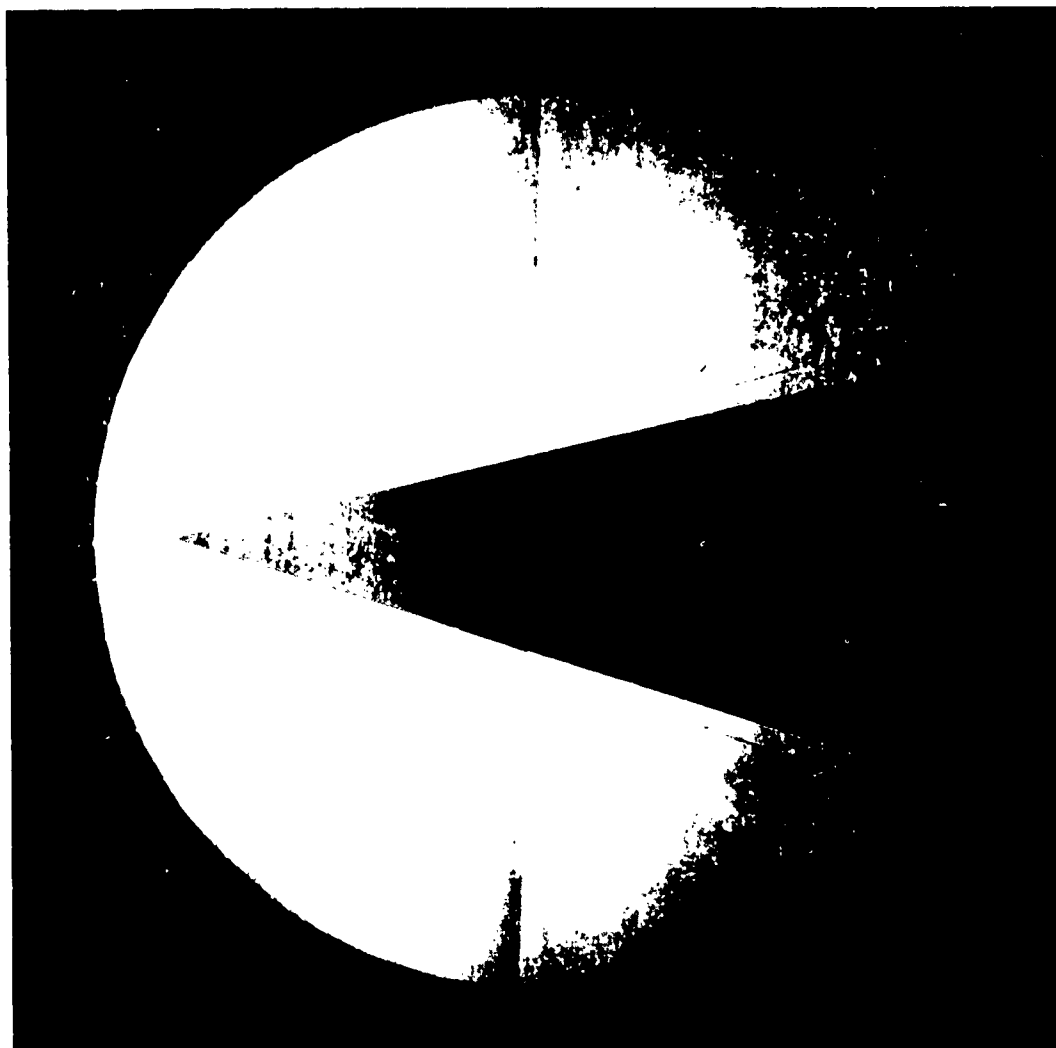
e. $\alpha = 40$ deg
Fig. 20 Continued



f. $\alpha \approx 50$ deg
Fig. 20 Continued

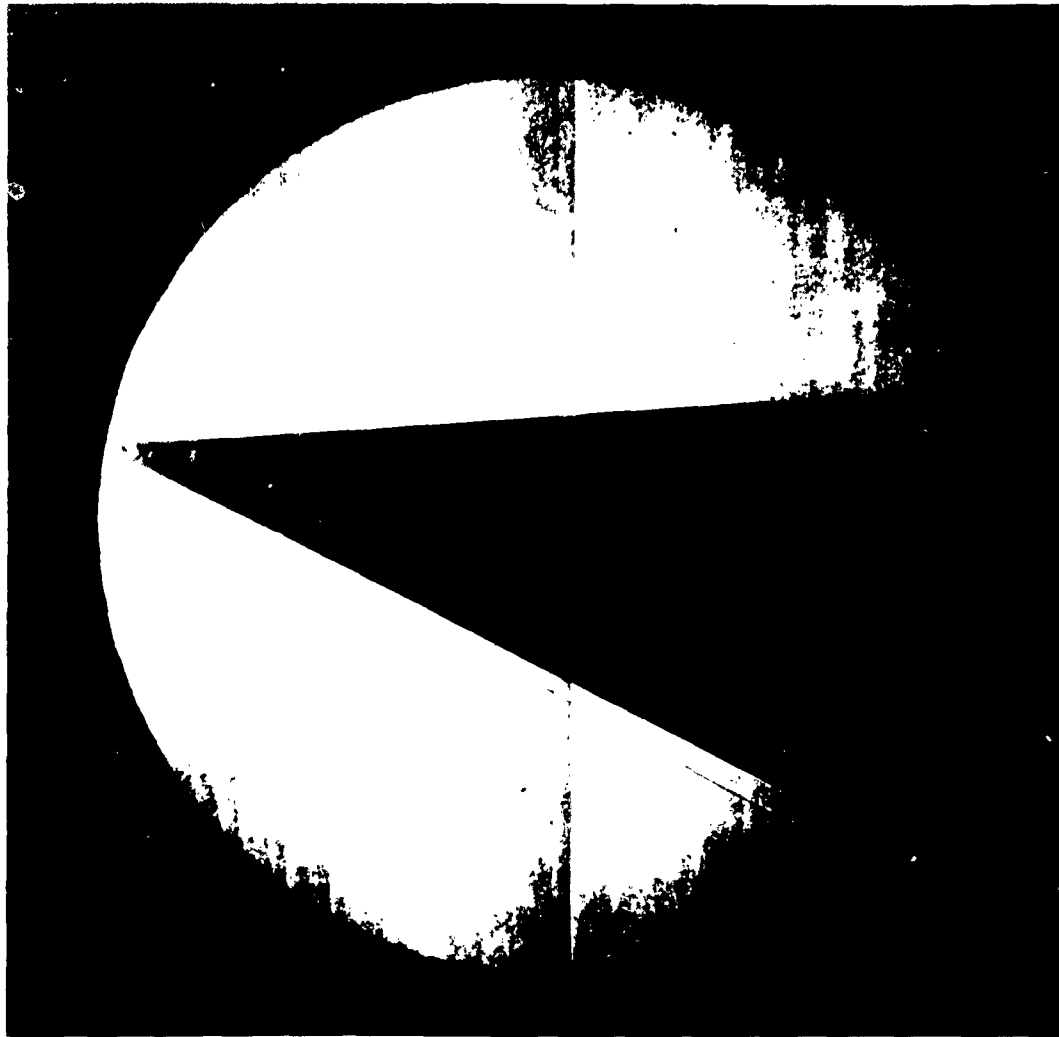


g. $\alpha = 60$ deg
Fig. 20 Concluded



a. $\alpha = 0 \text{ deg}$

Fig. 21 Shadowgraphs of Configuration 2



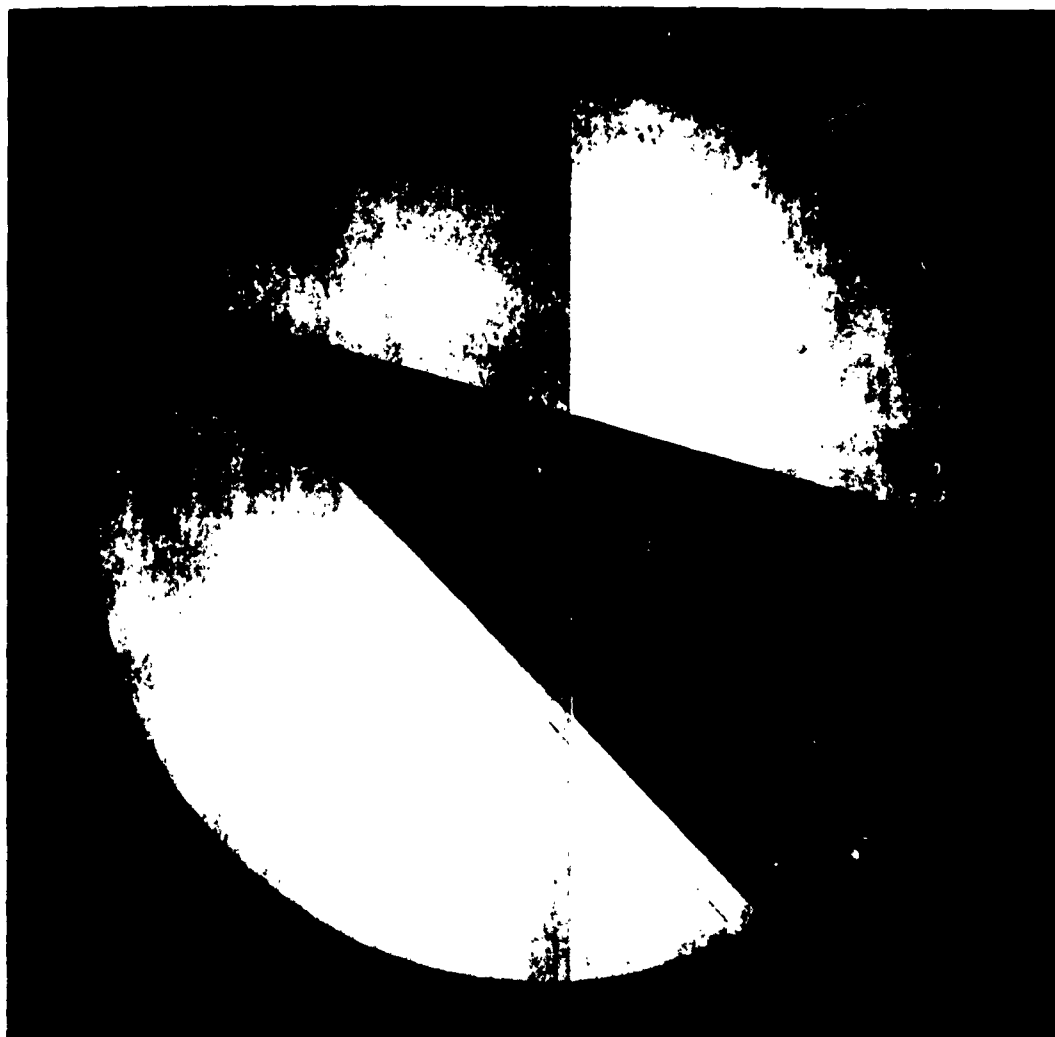
b. $\alpha = 10$ deg

Fig. 21 Continued

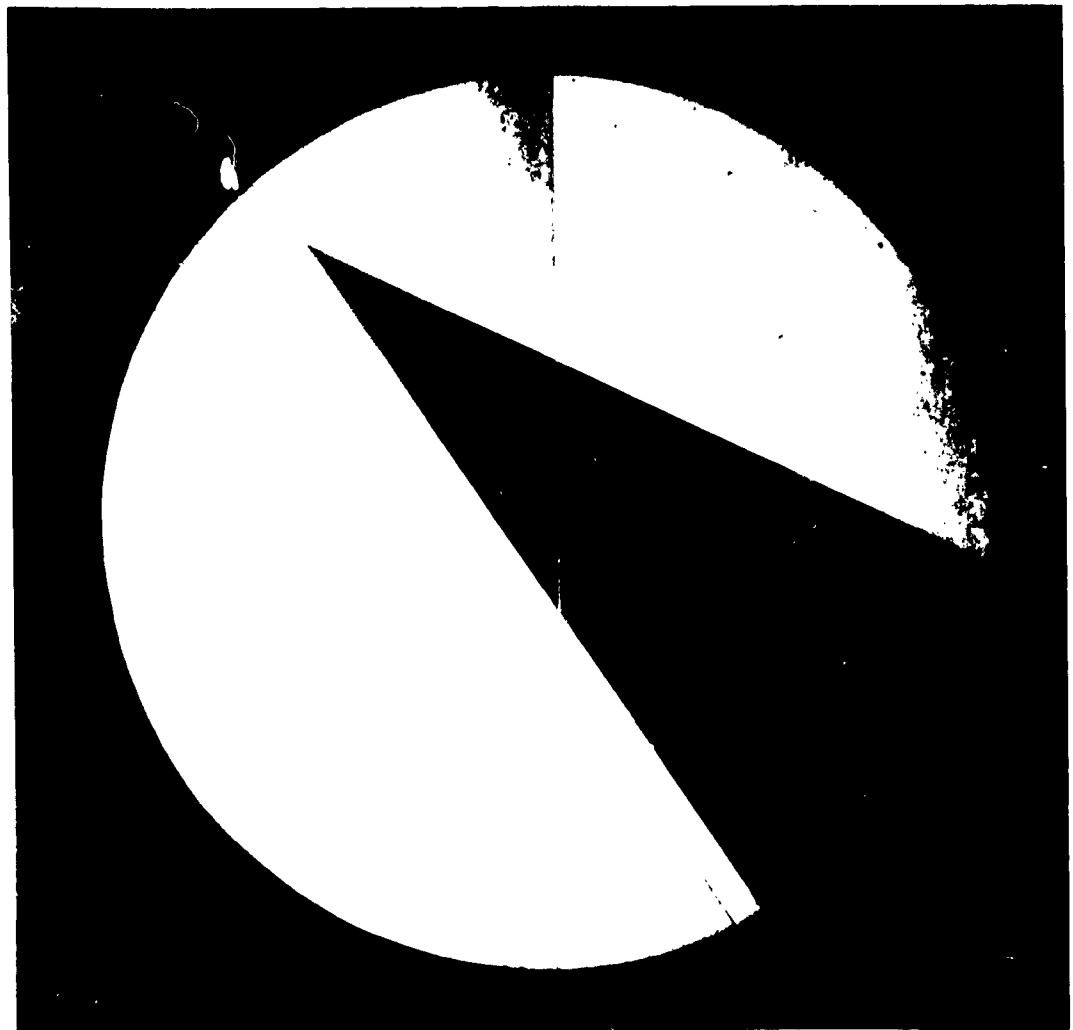


c. $\alpha = 20$ deg

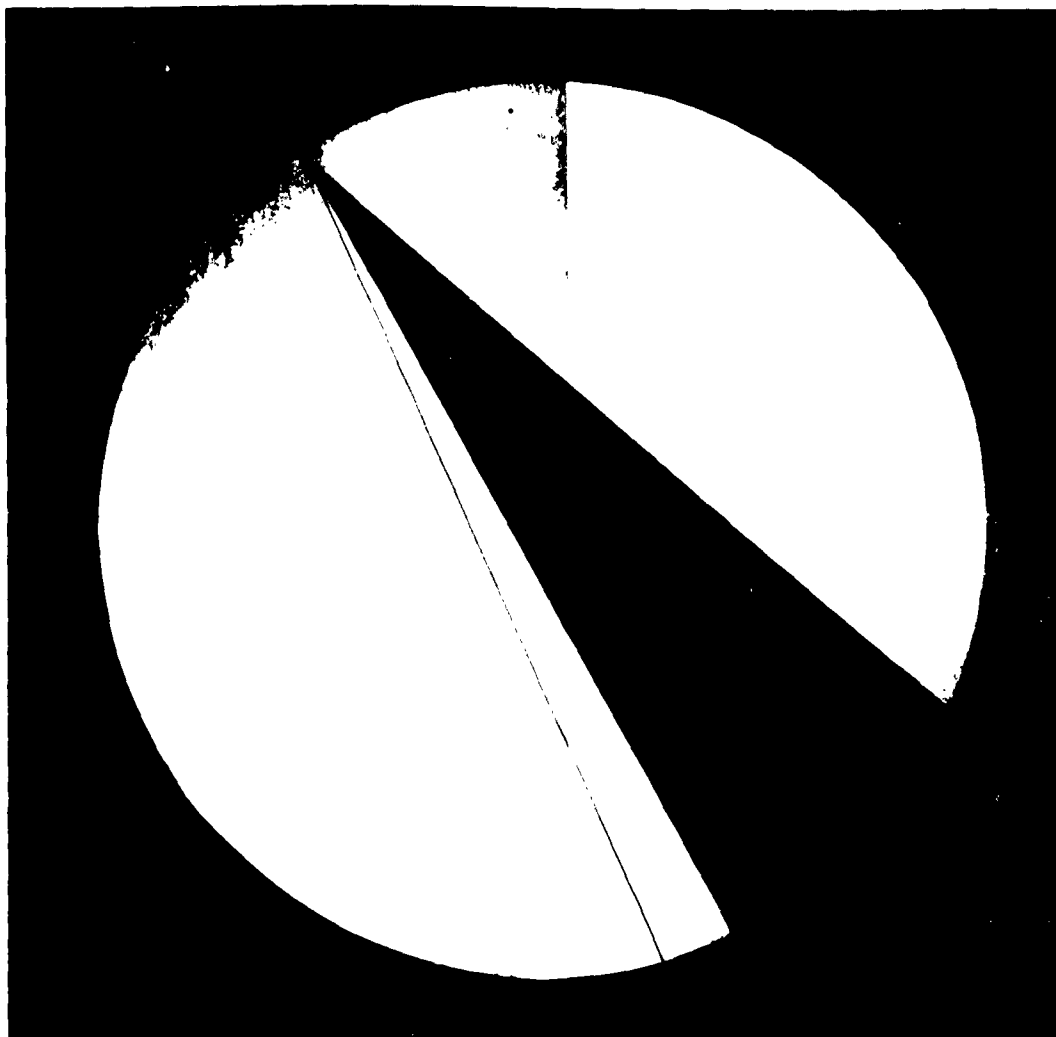
Fig. 21 Continued



d. $\alpha = 30$ deg
Fig. 21 Continued

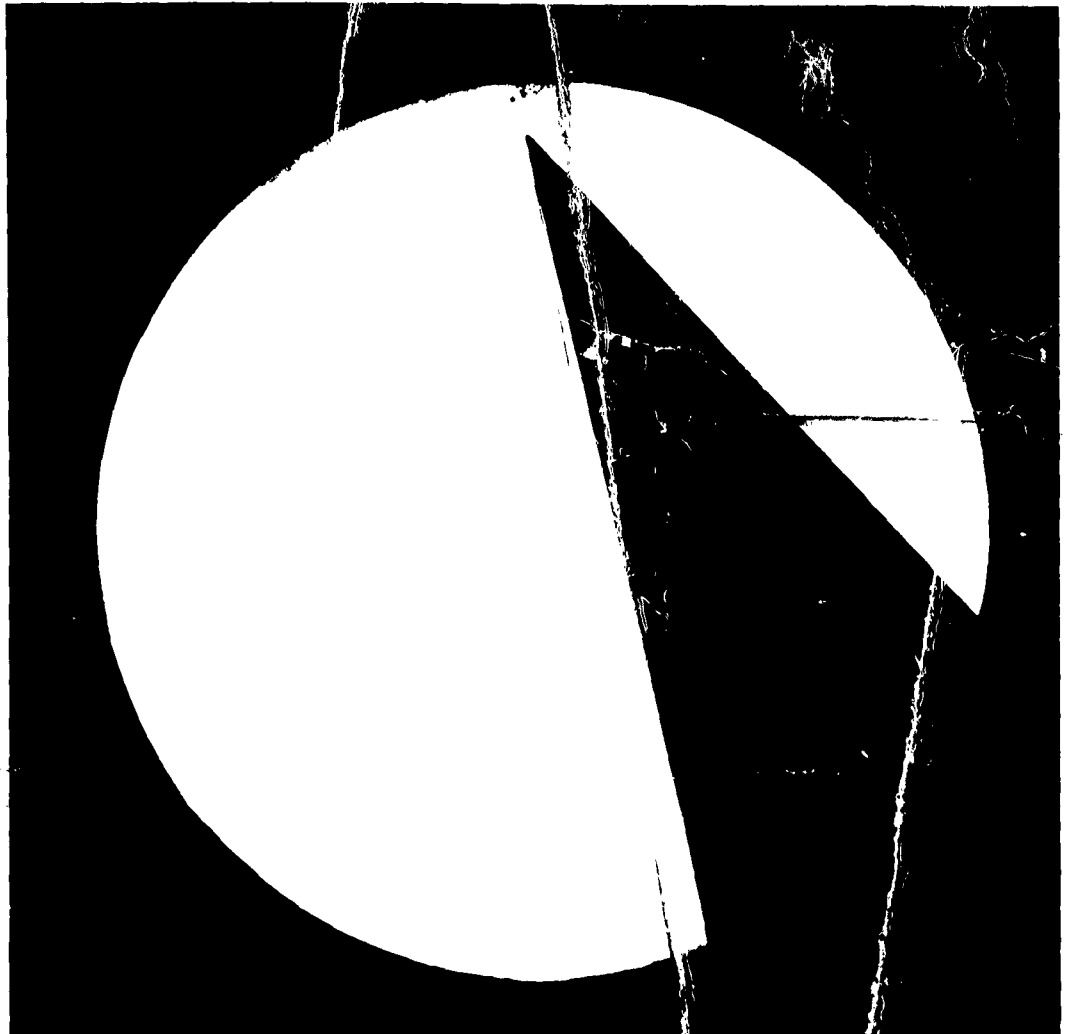


e. $\alpha = 40$ deg
Fig. 21 Continued



f. $\alpha \approx 50$ deg

Fig. 21 Continued



g. $\alpha \approx 60$ deg

Fig. 21 Concluded

FOR ERRATA

AD _____

414567

THE FOLLOWING PAGES ARE CHANGES

TO BASIC DOCUMENT

AD-414567

UNCLASSIFIED

Errata AEDC-TDR-63-163*, August 1963

Please note the following revisions:

1. The shadowgraph shown on page 44 as Fig. 20c should be Fig. 21c on page 51. The shadowgraph shown on page 51 as Fig. 21c should be Fig. 20c on page 44.
2. The shadowgraph shown on page 47 as Fig. 20f should be Fig. 21f on page 54. The shadowgraph shown on page 54 as Fig. 21f should be Fig. 20f on page 47.

*R. L. Palko and A. D. Ray. "Pressure Distribution and Flow Visualization Tests of a 1.5 Elliptic Cone at Mach 10." AEDC-TDR-63-163, August 1963.

UNCLASSIFIED

AD _____

414567

END CHANGE PAGES